Variable metric proximal stochastic gradient methods with additional sampling

Nataša Krklec Jerinkić[1], Federica Porta[2], Valeria Ruggiero[3] and Ilaria Trombini[3,4*]

[1]Faculty of Sciences, Department of Mathematics and Informatics, University of Novi Sad, Trg Dositeja Obradovića 4, Novi Sad, 21000, Serbia.
[2]Department of Physics, Informatics and Mathematics, University of Modena and Reggio Emilia, Via Campi 213A, Modena, 41125, Italy.
[3]Department of Mathematics and Computer Science, University of Ferrara, Via Machiavelli 30, Ferrara, 44121, Italy.
[4]Department of Mathematical, Physical and Computer Sciences, University of Parma, Parco Area delle Scienze, 7/A, Parma, 43124, Italy.

*Corresponding author(s). E-mail(s): ilaria.trombini@unife.it;
Contributing authors: natasa.krklec@dmi.uns.ac.rs;
federica.porta@unimore.it; rgv@unife.it;

Abstract

Regularized empirical risk minimization problems arise in a variety of applications, including machine learning, signal processing, and image processing. Proximal stochastic gradient algorithms are a standard approach to solve these problems due to their low computational cost per iteration and a relatively simple implementation. This paper introduces a class of proximal stochastic gradient methods built on three key elements: a variable metric underlying the iterations, a stochastic line search governing the decrease properties and an incremental mini-batch size technique based on additional sampling. Convergence results for the proposed algorithms are proved under different hypotheses on the function to minimize. No assumption is required regarding the Lipschitz continuity of the gradient of the differentiable part of the objective function. Possible strategies to automatically select the parameters of

the suggested scheme are discussed. Numerical experiments on binary classification problems show the effectiveness of the suggested approach compared to other state-of-the-art proximal stochastic gradient methods.

Keywords: Proximal stochastic gradient methods, Variable Metrics, Additional sampling, Machine Learning

MSC Classification: 65K05 , 90C15 , 62L20

1 Introduction

In this paper we are interested in solving the following composite optimization problem

$$\min_{x\in\mathbb{R}^d}\left\{H_{\mathcal{N}}(x) := f_{\mathcal{N}}(x) + R(x)\right\} \tag{1}$$

where $f_{\mathcal{N}}(x)$ is the average of many smooth component functions $f_i(x)$, i.e.,

$$f_{\mathcal{N}}(x) = \frac{1}{N}\sum_{i=1}^{N} f_i(x),$$

and R is a proper, lower semi-continuous and convex function, which may be non-differentiable. Problem (1) is often referred to as regularized empirical risk minimization [1] and it covers a broad range of applications in machine learning (see, e.g. [2–5]) as well as in signal and image processing [6, 7].

1.1 Proximal gradient methods

Proximal gradient methods are a standard approach to solve problem (1). Indeed this algorithm consists of a forward step, which leverages the differentiability of $f_{\mathcal{N}}$, and a backward step, which exploits the convexity of R. Given an initial point $x^{(0)} \in \mathbb{R}^d$, the simplest proximal gradient method (Prox-GD) is based on the following update rule

$$x^{(k+1)} = \operatorname{argmin}_{x\in\mathbb{R}^d}\left\{\nabla f_{\mathcal{N}}(x^{(k)})^T x + \frac{1}{2\alpha_k}\|x - x^{(k)}\|^2 + R(x)\right\}, \tag{2}$$

where α_k is a positive learning rate. By defining the proximal mapping of a convex function $R(\cdot)$ at $y \in \mathbb{R}^d$ as

$$\operatorname{prox}_R(y) = \operatorname{argmin}_{x\in\mathbb{R}^d}\left\{\frac{1}{2}\|x - y\|^2 + R(x)\right\},$$

the proximal gradient iteration (2) can be more compactly written as

$$x^{(k+1)} = \operatorname{prox}_{\alpha_k R}(x^{(k)} - \alpha_k \nabla f_{\mathcal{N}}(x^{(k)})). \tag{3}$$

Proximal gradient methods have been extensively studied, leading to various versions that incorporate features such as inertial steps, approximate computation of the proximal operator, variable metric strategies, and adaptive step-length selection rules (see, for example, [8–10], the survey [11] and references therein). Below, we outline the class of variable metric proximal gradient algorithm, suggested by several authors [12–16], which serves as a starting point for the method proposed in this paper. Given proper positive parameters α_k and t_k, a general variable metric proximal gradient method can be defined through the following update

$$\begin{cases} d^{(k)} = \text{prox}_{\alpha_k R}^{S_k}(x^{(k)} - \alpha_k S_k^{-1} \nabla f_{\mathcal{N}}(x^{(k)})) - x^{(k)} \\ x^{(k+1)} = x^{(k)} + t_k d^{(k)} \end{cases}. \tag{4}$$

Here, $\{S_k\} \subset \mathbb{R}^{d \times d}$ is a sequence of symmetric and positive definite scaling matrices, designed to capture some local features of the minimization problem without introducing significant additional computational costs. In this context, the proximity operator of a convex function αR for $\alpha > 0$, with respect to a symmetric and positive definite matrix S, is generalized as

$$\text{prox}_{\alpha R}^{S}(y) = \text{argmin}_{x \in \mathbb{R}^d} \left\{ \frac{1}{2} \|x - y\|_S^2 + \alpha R(x) \right\},$$

where $\| \cdot \|_S$ denotes the norm induced by S.

1.2 Proximal stochastic gradient methods

When the number of components N is very large, computing $f_{\mathcal{N}}$ and its gradient may become unfeasible from the practical point of view. For this reason, a proper estimator of $f_{\mathcal{N}}$ is typically considered leading to the class of proximal stochastic gradient descent (Prox-SGD) methods. The update formula for Prox-SGD algorithms reads as

$$x^{(k+1)} = \text{prox}_{\alpha_k R}(x^{(k)} - \alpha_k \nabla f_{\mathcal{N}_k}(x^{(k)})),$$

where $\mathcal{N}_k$ is a subset of $\mathcal{N}$ of size N_k, randomly and uniformly chosen at iteration k, and

$$f_{\mathcal{N}_k}(x) = \frac{1}{N_k} \sum_{i \in \mathcal{N}_k} f_i(x). \tag{5}$$

Hereafter $\mathcal{N}_k$ will be also referred to as mini-batch.

Prox-SGD offers an advantage over the Prox-GD scheme in (3) because it computes the gradient of only a relatively small number of randomly selected functions f_i at each iteration. However, for Prox-SGD to converge, its step-size must decrease to zero at an appropriate rate, resulting in a convergence rate of $\mathcal{O}(1/\sqrt{k})$ for $\mathbb{E}[H_{\mathcal{N}}(x^{(k)}) - H_{\mathcal{N}}(x^*)]$ [17]. Additionally, even when $H_{\mathcal{N}}(x)$ is

strongly convex, the convergence rate for Prox-SGD improves only to $\mathcal{O}(1/k)$ [18], which is significantly slower than the linear convergence rate achieved by Prox-GD.

To address the issue of diminishing step-size and slow convergence typical of standard stochastic gradient methods, either incremental techniques [19–25] or variance reduced strategies [26–32] have been proposed in the literature. Incremental stochastic gradient schemes are based on the idea of progressively increasing the mini-batch size over iterations, thereby employing increasingly accurate gradient estimates as the optimization process proceeds. The main limitations of such approaches are either the excessively rapid growth of the mini-batch size, as for the methods suggested in [20, 24], or the computationally expensive and memory demanding increasing conditions needed to be checked by the schemes proposed in [19, 21–23, 25]. On the other hand, variance reduced stochastic gradient algorithms require periodic computation of a full gradient (or an estimate based on a large mini-batch). For this reason, these approaches are generally not employed in applications involving large-scale datasets or deep neural networks.

Both incremental and variance reduced strategies allow to avoid vanishing sequences of learning rates, which are typically defined by a fixed value. Selecting this value is challenging, as it significantly impacts the numerical performance of the algorithms. Manual tuning of the learning rate through trial-and-error is common in this context, resulting in a high workload.

1.3 Contributions

The main aim of this paper is to develop a stochastic version of the variable metric proximal gradient method, as defined in (4), where the gradient of the approximation (5) is used in place of the gradient of $f_{\mathcal{N}}$. The main ingredients of the suggested approach are the following.

(i) *Flexibility in selecting α_k and S_k.* The convergence results provided for the suggested scheme hold under very general assumptions on the parameters α_k and S_k. This flexibility allows users to adopt the most appropriate strategy for defining both the learning rate and the sequence of scaling matrices in order to accelerate convergence. Different definitions of α_k and S_k result in different methods. Possible automatic and adaptive techniques to select α_k and S_k are discussed with the aim of avoiding manual parameter tuning. We stress that there is no requirement for the learning rate sequence to vanish.

(ii) *A stochastic Armijo-like line search to define t_k.* The additional parameter t_k is employed to ensure a sufficient reduction of the current stochastic approximation of the objective function (5) at each iteration. Examples of stochastic gradient schemes combined with line search procedures can also be found in [19, 22, 33–35]. However, in all of these works, the aim of the line search is to adjust the learning rate α_k and this approach can limit the flexibility of its selection. Moreover, since the starting value for t_k must be always set to 1 and then it is automatically and dynamically adjusted

via the line search, t_k does not introduce any additional parameters that need tuning. On the other hand, the numerical performance of the schemes proposed in [19, 22, 33–35] depends on a proper strategy for selecting the initial guess for the line search.

(iii) *A proper incremental strategy to select the mini-batch size based on an additional sampling.* The algorithm developed in this paper falls within the class of incremental stochastic gradient methods. In particular, the mini-batch size increases (or stays the same) with each iteration based on the so-called additional sampling, employed for example in [36, 37]. With the additional sampling, alongside the mini-batch $\mathcal{N}_k$ used for the line search on t_k, a second (randomly chosen) mini-batch is introduced to evaluate whether a reduction, or at least a controlled increase, in the stochastic approximation of the objective function, related to this second mini-batch, is also achieved. If this situation does not occur, the mini-batch size is appropriately increased, as the current size probably does not ensure a reduction in the true objective function. In the approach suggested in this paper, the additional sampling is used to determine whether or not to keep the same mini-batch fixed, not only its size. In this way different successive iteration of the optimization process are employed to efficiently minimize the same stochastic approximation of the objective function, while not excluding the possibility to reduce the true objective function due to the presence of additional sampling. The idea of keeping the same mini-batch fixed for a predetermined number of iterations has also been considered in [37, 38]. Nevertheless, our method differs from those in [36–38] for two main reasons: first, the algorithms in [36–38] are thought for objective functions which do not incorporate a regularization term; second, they do not use a variable metric to enhance the convergence of the schemes. Lastly, it is worth noting that the method proposed in [39] also employs additional sampling to control step acceptance and adjust the sample size when needed. However, it differs significantly from our approach, as it is based on the trust-region framework and utilizes Hessian approximations

For general objective functions, we prove that the limit points of the sequence generated by the proposed algorithm are almost surely stationary. Furthermore, we establish the almost sure convergence of both the sequence of the objective function values and the sequence of the iterates, given the additional assumptions of convexity and strong convexity for the objective function, respectively. All the convergence results hold without requiring the gradient of $f_{\mathcal{N}}$ to be Lipschitz continuous.

The suggested method has been applied to binary classification problems, demonstrating promising results compared to state-of-the-art algorithms, as well as robustness in parameter tuning.

1.4 Outline of the paper

The paper is organized as follows. In Section 2 we detail the structure of the general variable metric proximal stochastic gradient algorithm we are proposing. Moreover, a possibility to select both the learning rate and the scaling matrix is described. Finally the convergence results of the scheme are stated under different assumptions on the objective function. In Section 3 we report the results of the numerical experiments we carried out on two different regularized empirical risk minimization problems. Conclusions are presented in the final section, which also outlines directions for future work.

1.5 Notations

The following notations will be used throughout the paper.

- $\mathbb{R}_+$ is the set of non negative real numbers; $\mathbb{R}_{++}$ is the set of positive real numbers.
- $\|\cdot\|$ denotes the standard ℓ_2 norm. Given a symmetric and positive definite matrix S of order k, the S-norm of a vector $x \in \mathbb{R}^d$ is defined as $\|x\|_S \equiv \sqrt{x^T S x}$.
- Given $\mu \geq 1$, we denote by $\mathcal{M}_\mu$ the set of all symmetric positive definite matrices with all eigenvalues contained in the interval $[\frac{1}{\mu}, \mu]$.
- Let $D_1, D_2 \in \mathbb{R}^{d\times d}$ be symmetric and positive definite matrices. The notation $D_1 \succeq D_2$ indicates that $D_1 - D_2$ is a symmetric and positive semidefinite matrix or, equivalently, $x^T D_1 x \geq x^T D_2 x$ for any $x \in \mathbb{R}^d$.
- $\mathbb{E}[\cdot]$ and $\mathbb{E}[\cdot|\ \mathcal{F}]$ denote mathematical expectation and conditional expectation with respect to σ-algebra $\mathcal{F}$, respectively.
- We use "a.s." to abbreviate "almost sure/surely" and "i.i.d." to abbreviate "independent and identically distributed", while "SAA" stands for "sample average approximation".
- We denote by $|\mathcal{N}|$ the cardinality of set $\mathcal{N}$.
- Given a matrix $A \in \mathbb{R}^{d\times d}$, we denote by $\mathrm{diag}(A)$ the diagonal matrix whose diagonal elements are the diagonal elements of A.

2 The algorithm and its convergence analysis

In this section we present a variable metric proximal stochastic gradient method based on both the line search and the additional sampling. Moreover the convergence analysis of the scheme will be provided.

2.1 The algorithm

The method we suggest is based on the following iteration

$$\begin{cases} d_k^{(\mathcal{N}_k)} = v_k^{(\mathcal{N}_k)} - x_k = \mathrm{prox}_{\alpha_k R}^{S_k}(x_k - \alpha_k S_k^{-1} \nabla f_{\mathcal{N}_k}(x_k)) - x_k \\ x_{k+1} = x_k + t_k d_k^{(\mathcal{N}_k)}, \end{cases}$$

where

$\mathcal{N}_k$ is a randomly chosen subset of $\mathcal{N}$ of size N_k;
$\alpha_k \in \mathbb{R}$ is a positive learning rate such that $0 < \alpha_{min} \leq \alpha_k \leq \alpha_{max}$;
S_k is a symmetric and positive definite scaling matrix of size d;
$t_k \in (0, 1]$ is a line search parameter employed to ensure a sufficient decrease of the current approximation $H_{\mathcal{N}_k}(x) = f_{\mathcal{N}_k}(x) + R(x)$ of the objective function. Indeed, starting from $t_k = 1$, it is reduced by a factor $\beta \in (0, 1)$ until the following condition is met

$$H_{\mathcal{N}_k}(x_k + t_k d_k) \leq H_{\mathcal{N}_k}(x_k) + \eta t_k q_{\mathcal{N}_k}(v_k^{(\mathcal{N}_k)}), \tag{6}$$

where

$$q_{\mathcal{N}_k}^{\alpha_k, S_k}(y) = (y - x_k)^T \nabla f_{\mathcal{N}_k}(x_k) + \frac{1}{2\alpha_k}\|y - x_k\|_{S_k}^2 + R(y) - R(x_k) \tag{7}$$

and $\eta \in (0, 1)$. It is immediate to prove that (6) ensures a reduction of $H_{\mathcal{N}_k}(\cdot)$ moving from x_k to $x_k + t_k d_k$ since $q_{\mathcal{N}_k}^{\alpha_k, S_k}(v_k^{(\mathcal{N}_k)})$ is non-positive. Indeed seeing that

$$\begin{aligned} v_k^{(\mathcal{N}_k)} &= \text{prox}_{\alpha_k R}^{S_k}(x_k - \alpha_k S_k^{-1} \nabla f_{\mathcal{N}_k}(x_k)) \\ &= \text{argmin}_{y \in \mathbb{R}^d} R(y) + \frac{1}{2\alpha_k}\|y - (x_k - \alpha_k S_k^{-1} \nabla f_{\mathcal{N}_k}(x_k))\|_{S_k}^2 \\ &= \text{argmin}_{y \in \mathbb{R}^d}\ q_{\mathcal{N}_k}^{\alpha_k, S_k}(y) + R(x_k) + \frac{\alpha_k}{2}\|\nabla f_{\mathcal{N}_k}(x_k)\|_{S_k}^2 \\ &= \text{argmin}_{y \in \mathbb{R}^d}\ q_{\mathcal{N}_k}^{\alpha_k, S_k}(y) \end{aligned}$$

the following inequality holds:

$$q_{\mathcal{N}_k}^{\alpha_k, S_k}(v_k^{(\mathcal{N}_k)}) \leq q_{\mathcal{N}_k}^{\alpha_k, S_k}(x_k) = 0.$$

It is well known that the function $q_{\mathcal{N}_k}^{\alpha_k, S_k}(\cdot)$ enjoys several properties that are recalled in Appendix A.

However, the update x_{k+1} is accepted only if it is able to ensure a sufficient decrease (or, at most, a controlled increase) of another approximation of the objective function computed on a different subsample. In more detail, given a different subsample $\mathcal{D}_k$ randomly chosen from $\mathcal{N}$, the following checking condition is controlled:

$$H_{\mathcal{D}_k}(x_k + t_k d_k^{(\mathcal{N}_k)}) \leq H_{\mathcal{D}_k}(x_k) + c_{min} q_{\mathcal{D}_k}^{\bar{\alpha}}(v_k^{(\mathcal{D}_k)}) + C_{max}\zeta_k, \tag{8}$$

where, similarly to (7),

$$q_{\mathcal{D}_k}^{\bar{\alpha}}(y) = (y - x_k)^T \nabla f_{\mathcal{D}_k}(x_k) + \frac{1}{2\bar{\alpha}}\|y - x_k\|^2 + R(y) - R(x_k) \tag{9}$$

and $v_k^{(\mathcal{D}_k)} = \text{prox}_{\bar{\alpha}R}(x_k - \bar{\alpha}\nabla f_{\mathcal{D}_k}(x_k))$ with $\bar{\alpha} \in [\alpha_{min}, \alpha_{max}]$. The parameters c_{min} and C_{max} are positive real scalars and $\{\zeta_k\}$ is a summable sequence of non-negative real numbers. We remark that for the checking condition (9) we use a non-scaled gradient direction.

If condition (8) is not met the vector $x_k + t_k d_k^{(\mathcal{N}_k)}$ is rejected, $x_{k+1} = x_k$ and a new mini-batch $\mathcal{N}_{k+1}$ of larger size $N_{k+1} \in (N_k, N]$ is considered. Conversely, when the additional condition (8) is satisfied, then $x_{k+1} = x_k + t_k d_k^{(\mathcal{N}_k)}$ is accepted, and the optimization algorithm continues using the same approximation of the objective function, meaning that the mini-batch remains unchanged. Actually if the mini-batch remains unchanged for a predetermined number of iterations, a new mini-batch is randomly selected from $\mathcal{N}$, keeping the same cardinality as for the previous mini-batch. The main steps of the proposed approach are detailed in Algorithm 1 and described below.

Step 1 is devoted to the selection of a positive step-length, belonging to a bounded and closed interval, and a symmetric and positive definite scaling matrix with bounded eigenvalues. Possible strategies to define these parameters are discussed in Section 2.3.

Step 2 aims at computing the proximal stochastic gradient direction given the mini-batch $\mathcal{N}_k$, the scaling matrix S_k and the learning rate α_k. If $q_{\mathcal{N}_k}^{\alpha_k, S_k}(v_k^{(\mathcal{N}_k)})$ is equal to zero, namely x_k is a stationary point for $H_{\mathcal{N}_k}$ (see item d. of Lemma A.1), then the mini-batch is changed.

Step 3 consists in the line search procedure on the parameter t_k. Until the sufficient decrease of the current approximation $H_{\mathcal{N}_k}$ of the objective function is not ensured in terms of (6), t_k is reduced by a factor $\beta < 1$. Lemma 2.1 guarantees that the line search is well defined.

Step 4 checks if the algorithm reaches the deterministic setting (namely $N_k = N$) or not. Particularly, if $N_k = N$ then Step 5, Step 6 and Step 7 are avoided since they only refer to the stochastic scenario. We highlight that the first four steps of Algorithm 1 with $N_k = N$ reduce to a deterministic variable metric proximal gradient method with line search (see for example [12]).

Step 5 implements the additional sampling. A different sub-sample $\mathcal{D}_k$ is considered in order to verify if the attempt vector $x_k + t_k d_k^{(\mathcal{N}_k)}$ also guarantees a sufficient decrease of the different approximation $H_{\mathcal{D}_k}$ of the objective function. If condition (8) is verified, the algorithm trusts $x_k + t_k d_k^{(\mathcal{N}_k)}$ and the mini-batch is kept fixed for the next iteration provided that the prefixed number $m(N_k)$ of iterations with the same mini-batch has not been reached (see also Step 6). Indeed, the support variable $flag$ counts the number of iterations performed with the same mini-batch. If $flag > m(N_k)$ then a new mini-batch of the same size is considered. Otherwise, if the additional sampling condition (8) does not hold, the attempt vector computed in Step 1, Step 2 and Step 3 is rejected and the cardinality for the successive mini-batch is increased. When $d_k^{(\mathcal{N}_k)}$ satisfies (8), the reduction of $H_{\mathcal{D}_k}$, although relaxed by the presence of $C_{max}\zeta_k \geq 0$, can be considered as an indication that the decrease of $H_{\mathcal{N}_k}$ is acceptable in order to minimize the original objective function. In view of

Algorithm 1 Proximal Stochastic gradient method with Additional sampling and variable Metric (**Prox-SAM**)

Fix $x_0 \in \mathbb{R}^d$, $\eta, \beta \in (0,1)$, $\{\zeta_k\} \subset \mathbb{R}_+$ subject to $\sum_{k=0}^{\infty} \zeta_k \leq \overline{\zeta} < \infty$, c_{min}, $C_{max} \in \mathbb{R}_{++}$, $0 < \alpha_{min} < \alpha_{max}$, $\bar{\alpha} \in [\alpha_{min}, \alpha_{max}]$, $\mu \geq 1$, $N_0 > 0$, $\mathcal{N}_0 \subseteq \mathcal{N}$ of size N_0, $m(N_0) > 0$, $flag = 0$.

for $k = 0, 1, \ldots$ **do**

STEP 1. *Parameters selection*
Set $\alpha_k \in [\alpha_{min}, \alpha_{max}]$.
Set $S_k \in \mathcal{M}_\mu$.

STEP 2. *Computation of a scaled stochastic direction*
$v_k^{(\mathcal{N}_k)} = \text{prox}_{\alpha_k R}^{S_k}(x_k - \alpha_k S_k^{-1} \nabla f_{\mathcal{N}_k}(x_k))$
$d_k^{(\mathcal{N}_k)} = v_k^{(\mathcal{N}_k)} - x_k$
IF $q_{\mathcal{N}_k}^{\alpha_k, S_k}(v_k^{(\mathcal{N}_k)}) == 0$
THEN $N_{k+1} = N_k$, $flag = 0$ and go to STEP 7.
ELSE Set $t_k = 1$ and go to STEP 3.

STEP 3. *Line search procedure*
IF $H_{\mathcal{N}_k}(x_k + t_k d_k^{(\mathcal{N}_k)}) \leq H_{\mathcal{N}_k}(x_k) + \eta t_k q_{\mathcal{N}_k}^{\alpha_k, S_k}(v_k^{(\mathcal{N}_k)})$
THEN $\overline{x}_k = x_k + t_k d_k^{(\mathcal{N}_k)}$ and go to STEP 4.
ELSE $t_k = t_k \cdot \beta$ and repeat STEP 3.

STEP 4. *Check for deterministic or stochastic setting*
IF $N_k < N$
THEN go to STEP 5.
ELSE $x_{k+1} = \overline{x}_k$ and go to STEP 1.

STEP 5. *Additional sampling*
Choose $\mathcal{D}_k$ randomly and uniformly from $\mathcal{N}$ with replacement.
$v_k^{(\mathcal{D}_k)} = \text{prox}_{\bar{\alpha} R}(x_k - \bar{\alpha} \nabla f_{\mathcal{D}_k}(x_k))$
$d_k^{(\mathcal{D}_k)} = v_k^{(\mathcal{D}_k)} - x_k$
IF $H_{\mathcal{D}_k}(\overline{x}_k) \leq H_{\mathcal{D}_k}(x_k) + c_{min} q_{\mathcal{D}_k}^{\bar{\alpha}}(v_k^{(\mathcal{D}_k)}) + C_{max}\zeta_k$
THEN $x_{k+1} = \overline{x}_k$, $N_{k+1} = N_k$, $flag = flag + 1$ and go to STEP 6.
ELSE $x_{k+1} = x_k$, $N_{k+1} \in (N_k, N]$, $flag = 0$ and go to STEP 7.

STEP 6. *Check for keeping the same mini-batch*
IF $flag < m(N_k)$
THEN go to STEP 1.
ELSE $flag = 0$ and go to STEP 7.

STEP 7. *Sample selection*
Randomly choose $\mathcal{N}_{k+1} \subseteq \mathcal{N}$ of size N_{k+1}.
Compute the possible maximum number $m(N_{k+1})$ of iterations with the same mini-batch.

end for

$\sum_{k=0}^{\infty} \zeta_k < \infty$, we have $\zeta_k \to 0$, so that the condition (8) becomes stricter as k increases. Furthermore, we highlight that there are no conditions on the size of $\mathcal{D}_k$, i.e., $\mathcal{D}_k$ can consist of only one element. Finally, we stress that if condition (8) fails to be satisfied for many iterations, as the size of the mini-batch is increased, there exists an iteration $\overline{k}$ such that, for $k \geq \overline{k}$, $N_k = N$ and

the method is switched to a deterministic proximal gradient method combined with a line search.

Step 6 verifies if the same mini-batch has been already employed for $m(N_k)$ iterations.

Step 7 performs a new mini-batch selection. This step is reached only if either the additional sampling failed (namely $\bar{x}_k$ ensures a decrease only for $H_{\mathcal{N}_k}$) or the same mini-batch has been considered for $m(N_k)$ successive iterations. We remark that $m(N_k)$ can change along the iterative process.

We remark that it is possible to add a stopping criterion. Specifically, a stopping criterion should be checked before the procedure returns to Step 1.

2.2 The convergence analysis

Assumption 1. The non-negative real sequence $\{\zeta_k\}$ in (8) is such that $\sum_{k=0}^{\infty} \zeta_k \leq \overline{\zeta}$.

Assumption 2. There exists $\bar{H}_{\mathcal{N}} \in \mathbb{R}$ such that $H_{\mathcal{N}}(x) \geq \bar{H}_{\mathcal{N}}$, $\forall x \in \mathbb{R}^d$.

The first lemma regards some properties of the line search in Step 4 of Algorithm 1.

Lemma 2.1. *If the function $f_{\mathcal{N}}(\cdot)$ in (1) is continuously differentiable and the function $R(\cdot)$ in (1) is convex, then the line search procedure in* Step 3 *of Algorithm 1 is well defined.*

Proof The proof of this lemma is identical to the one of [12, Proposition 3.1]. However we report in Appendix A the main arguments for the sake of completeness. □

Let us denote by $\mathcal{D}_k^+$ the subset of all possible outcomes of $\mathcal{D}_k$ at iteration k for which the condition (8) is satisfied, i.e.,

$$\mathcal{D}_k^+ = \{\mathcal{D}_k \subset \mathcal{N} \mid H_{\mathcal{D}_k}(\overline{x}_k) \leq H_{\mathcal{D}_k}(x_k) + c_{min} q_{\mathcal{D}_k}^{\bar{\alpha}}(v_k^{(\mathcal{D}_k)}) + C_{max}\zeta_k\}. \quad (10)$$

We denote the complementary subset of outcomes at iteration k by

$$\mathcal{D}_k^- = \{\mathcal{D}_k \subset \mathcal{N} \mid H_{\mathcal{D}_k}(\overline{x}_k) > H_{\mathcal{D}_k}(x_k) + c_{min} q_{\mathcal{D}_k}^{\bar{\alpha}}(v_k^{(\mathcal{D}_k)}) + C_{max}\zeta_k\}. \quad (11)$$

The first lemma guarantees that if the mini-batches are always proper subsets of $\mathcal{N}$, then from a certain iteration forward the SD condition is always satisfied. The proof can be found in Appendix A.3 since its arguments are the same of the proofs of [37, Lemma 1] and [39, Lemma 1].

Lemma 2.2. *Suppose that Assumption 1 holds. If $N_k < N$ for all $k \in \mathbb{N}$, then a.s. there exists $k_1 \in \mathbb{N}$ such that $\mathcal{D}_k^- = \emptyset$ for all $k \geq k_1$.*

Next, we show that Lemma 2.2 implies that the Armijo-like inequality (8) holds for the overall objective function for all k sufficiently large in the mini-batch scenario. The proof is similar to the one of Lemma 2 in [39].

Lemma 2.3. *Suppose that Assumption 1 holds. If $N_k < N$ for all $k \in \mathbb{N}$, then, given $\bar{\alpha} > 0$ and $v_k^{(i)} = \mathrm{prox}_{\bar{\alpha}R}(x_k - \bar{\alpha}\nabla F_i(x_k))$,*

$$H_{\mathcal{N}}(\bar{x}_k) \leq H_{\mathcal{N}}(x_k) - \frac{c_{min}}{2\bar{\alpha}} \frac{1}{N} \sum_{i=1}^{N} \|x_k - v_k^{(i)}\|^2 + C_{max}\zeta_k,$$

holds a.s. for all $k \geq k_1$ where k_1 is as in Lemma 2.2.

Proof We first prove that the following inequality

$$q_{\mathcal{D}_k}^{\bar{\alpha}}(v_k^{(\mathcal{D}_k)}) \leq -\frac{1}{2\bar{\alpha}} \|v_k^{(\mathcal{D}_k)} - x_k\|^2 \tag{12}$$

holds true. In view of the definition of $v_k^{(\mathcal{D}_k)} = \mathrm{prox}_{\bar{\alpha}R}(x_k - \bar{\alpha}\nabla f_{\mathcal{D}_k}(x_k))$, it follows that

$$\frac{1}{\bar{\alpha}}(x_k - \bar{\alpha}\nabla f_{\mathcal{D}_k}(x_k) - v_k^{(\mathcal{D}_k)}) \in \partial R(v_k^{(\mathcal{D}_k)}). \tag{13}$$

Now we state an inequality for the elements of $\partial R(v_k^{(\mathcal{D}_k)})$. Indeed, for any $w \in \partial R(v_k^{(\mathcal{D}_k)})$ we have

$$\begin{aligned} q_{\mathcal{D}_k}^{\bar{\alpha}}(v_k^{(\mathcal{D}_k)}) &= \nabla f_{\mathcal{D}_k}(x_k)^T (v_k^{(\mathcal{D}_k)} - x_k) + \frac{1}{2\bar{\alpha}} \|v_k^{(\mathcal{D}_k)} - x_k\|^2 + \\ &\quad + R(v_k^{(\mathcal{D}_k)}) - R(x_k) \\ &\leq \nabla f_{\mathcal{D}_k}(x_k)^T (v_k^{(\mathcal{D}_k)} - x_k) + \frac{1}{2\bar{\alpha}} \|v_k^{(\mathcal{D}_k)} - x_k\|^2 + w^T (v_k^{(\mathcal{D}_k)} - x_k) \end{aligned}$$

Hence the previous inequality holds true for $\frac{1}{\bar{\alpha}}(x_k - \bar{\alpha}\nabla f_{\mathcal{D}_k}(x_k) - v_k^{(\mathcal{D}_k)})$ (see (13)). This results in

$$\begin{aligned} q_{\mathcal{D}_k}^{\bar{\alpha}}(v_k^{(\mathcal{D}_k)}) &\leq \nabla f_{\mathcal{D}_k}(x_k)^T (v_k^{(\mathcal{D}_k)} - x_k) + \frac{1}{2\bar{\alpha}} \|v_k^{(\mathcal{D}_k)} - x_k\|^2 + \\ &\quad + \frac{1}{\bar{\alpha}}(x_k - \bar{\alpha}\nabla f_{\mathcal{D}_k}(x_k) - v_k^{(\mathcal{D}_k)})^T (v_k^{(\mathcal{D}_k)} - x_k) \\ &= -\frac{1}{2\bar{\alpha}} \|v_k^{(\mathcal{D}_k)} - x_k\|^2 \end{aligned}$$

Lemma 2.2, together with (12), implies that a.s.

$$\begin{aligned} H_{\mathcal{D}_k}(\bar{x}_k) &\leq H_{\mathcal{D}_k}(x_k) + c_{min} q_{\mathcal{D}_k}^{\bar{\alpha}}(v_k^{(\mathcal{D}_k)}) + C_{max}\zeta_k \\ &\leq H_{\mathcal{D}_k}(x_k) - \frac{c_{min}}{2\bar{\alpha}} \|v_k^{(\mathcal{D}_k)} - x_k\|^2 + C_{max}\zeta_k \end{aligned} \tag{14}$$

holds for all possible realizations of $\mathcal{D}_k$ and for all $k \geq k_1$. Thus, we conclude that for every $i = 1, 2, ..., N$ and every $k \geq k_1$ a.s. we have

$$H_i(\bar{x}_k) \leq H_i(x_k) - \frac{c_{min}}{2\bar{\alpha}} \|v_k^{(i)} - x_k\|^2 + C_{max}\zeta_k,$$

where $H_i(x) = F_i(x) + R(x)$ and $v_k^{(i)} = \mathrm{prox}_{\bar{\alpha}R}(x_k - \bar{\alpha}\nabla F_i(x_k))$. Indeed, if there exists $i \in \mathcal{N}$ that violates the previous inequality, then there would exist at least

one realization of $\mathcal{D}_k$ (namely, $\mathcal{D}_k = \{i, i, ..., i\}$) that violates (14). Thus, a.s., for all $k \geq k_1$ we have

$$H_{\mathcal{N}}(\bar{x}_k) = \frac{1}{N}\sum_{i=1}^{N} H_i(\bar{x}_k) \leq \frac{1}{N}\sum_{i=1}^{N}(H_i(x_k) - \frac{c_{min}}{2\bar{\alpha}}\|v_k^{(i)} - x_k\|^2 + C_{max}\zeta_k)$$
$$= H_{\mathcal{N}}(x_k) - \frac{c_{min}}{2\bar{\alpha}}\frac{1}{N}\sum_{i=1}^{N}\|v_k^{(i)} - x_k\|^2 + C_{max}\zeta_k.$$

□

Theorem 2.1. *Suppose that the Assumptions 1 and 2 hold and $N_k < N$, for all $k \in \mathbb{N}$. Let $\{x_k\}$ be a sequence generated by Algorithm 1. Then, a.s., any limit point of the sequence $\{x_k\}$ is a stationary point for problem (1).*

Proof Lemma 2.3 and $\bar{\alpha} \in [\alpha_{min}, \alpha_{max}]$ imply that there exists $k_1 \in \mathbb{N}$ such that a.s. the following inequality holds for all $k \geq k_1$

$$H_{\mathcal{N}}(x_{k+1}) = H_{\mathcal{N}}(\bar{x}_k) \leq H_{\mathcal{N}}(x_k) - \frac{c_{min}}{2\alpha_{max}}\frac{1}{N}\sum_{i=1}^{N}\|x_k - v_k^{(i)}\|^2 + C_{max}\zeta_k, \quad (15)$$

where the equality comes from the fact that $\mathcal{D}_k^- = \emptyset$ and thus the candidate point is accepted. By subtracting $\bar{H}_{\mathcal{N}}$ to both members of the previous inequality and applying the conditional expected value with respect to the σ-algebra generated by $k_1, \ldots, k$ we get

$$\mathbb{E}\left[H_{\mathcal{N}}(x_{k+1}) - \bar{H}_{\mathcal{N}} \mid \mathcal{F}_{k_1}^k\right] \leq H_{\mathcal{N}}(x_k) - \bar{H}_{\mathcal{N}} +$$
$$- \frac{c_{min}}{2\alpha_{max}}\frac{1}{N}\sum_{i=1}^{N}\|x_k - v_k^{(i)}\|^2 + C_{max}\zeta_k.$$

where $\mathcal{F}_{k_1}^k$ denotes the the σ-algebra generated by $k_1, \ldots, k$. We note that both $x^{(k)}$ and $v_k^{(i)}$ do not depend on $\mathcal{N}_k$ and hence are $\mathcal{F}_{k_1}^k$-measurable. In view of the Robbins-Siegmund lemma [40, Lemma 11], we can conclude that

$$\sum_{k=k_1}^{+\infty}\sum_{i=1}^{N}\|x_k - v_k^{(i)}\|^2 < +\infty, \quad a.s.$$

and, hence,

$$\lim_{k\to+\infty}\sum_{i=1}^{N}\|x_k - v_k^{(i)}\|^2 = 0, \quad a.s.$$

As a consequence, we claim that $\forall i = 1, \ldots, N$,

$$\lim_{k\to+\infty}\|x_k - v_k^{(i)}\|^2 = 0, \quad a.s. \quad (16)$$

Let us suppose that there exists a subsequence of $\{x_k\}$ that converges a.s. to $\bar{x}$, namely there exists $\mathcal{K} \subseteq \mathbb{N}$ such that

$$\lim_{k\to\infty,\, k\in\mathcal{K}} x_k = \bar{x} \text{ a.s.}$$

Moreover, the continuity of both the proximal operator and $\nabla f_i(\cdot)$ with respect to all their arguments, implies that, in view of (16),

$$\lim_{k\to\infty,\, k\in\mathcal{K}} v_k^{(i)} = \mathrm{prox}_{\bar{\alpha}R}(\bar{x} - \bar{\alpha}\nabla f_i(\bar{x})) = \bar{x}, \quad \forall i = 1, \ldots, N.$$

As a consequence, $-\nabla f_i(\bar{x}) \in \partial R(\bar{x})$, $\forall i = 1, \ldots, N$, and due to convexity of the subdifferential we conclude that $-\nabla f_{\mathcal{N}}(\bar{x}) = -\frac{1}{N}\sum_{i=1}^{N} \nabla f_i(\bar{x}) \in \partial R(\bar{x})$, namely that $\bar{x}$ is a stationary point for $H_{\mathcal{N}}$ a.s.

□

By considering additional assumptions on the objective function, the convergence of both the sequence of the objective function values and the sequence of the iterates can be proved.

Theorem 2.2. *Suppose that the Assumptions 1 and 2 hold, $N_k < N$ for all $k \in \mathbb{N}$, and the objective function is convex. If the sequence $\{x_k\}$ generated by Algorithm 1 is bounded, then, a.s., the sequence of the objective function values $\{H_{\mathcal{N}}(x_k)\}$ converges to the minimum value $H_{\mathcal{N}}^*$ of $H_{\mathcal{N}}$.*

Proof By subtracting $H_{\mathcal{N}}^*$ to both sides of (15), the Robbins-Siegmund lemma implies that there exists a positive random variable Z such that $\{H_{\mathcal{N}}(x_k) - H_{\mathcal{N}}^*\}$ a.s. converges to Z. Since the sequence $\{x_k\}$ is bounded, it admits a subsequence $\{x_{k_j}\}$ that converges to some $\bar{x}$, which, according to the previous theorem, is a stationary point. Since the objective function is convex, $\bar{x}$ is a minimum point and $H_{\mathcal{N}}(\bar{x}) = H_{\mathcal{N}}^*$. By the continuity of $H_{\mathcal{N}}$, it follows that $H_{\mathcal{N}}(x_{k_j})$ converges to $H_{\mathcal{N}}(\bar{x}) = H_{\mathcal{N}}^*$. We can conclude that $Z = 0$ and that $\{H_{\mathcal{N}}(x_k)\}$ converges to $H_{\mathcal{N}}^*$ a.s. □

Theorem 2.3. *Suppose that the Assumptions 1 and 2 hold, $N_k < N$ for all $k \in \mathbb{N}$, and the objective function is $\mu_{\mathcal{N}}$-strongly convex. If the sequence $\{x_k\}$ generated by Algorithm 1 is bounded, then, a.s., $\{x_k\}$ converges to the unique solution x^* of problem (1).*

Proof If $H_{\mathcal{N}}$ is $\mu_{\mathcal{N}}$-strongly convex, problem (1) has a unique solution x^*. By denoting with $H_{\mathcal{N}}^*$ the value of the objective function in the solution, namely $H_{\mathcal{N}}(x^*) = H_{\mathcal{N}}^*$, in view of the strong convexity assumption for $H_{\mathcal{N}}$, the following inequality holds for any $x \in \mathbb{R}^d$:

$$\frac{\mu_{\mathcal{N}}}{2}\|x - x^*\|^2 \leq H_{\mathcal{N}}(x) - H_{\mathcal{N}}^*. \tag{17}$$

Since the sequence $\{x_k\}$ is bounded, Theorem 2.2 ensures that the sequence $\{H_{\mathcal{N}}(x_k) - H_{\mathcal{N}}^*\}$ converges to zero. As a consequence, taking x_k instead of x in (17) and letting $k \to \infty$, we obtain the convergence of the sequence generated by the algorithm to the unique solution x_* of problem (1). □

Theorem 2.4. *Suppose that the Assumption 2 holds and the full sample is reached. Then, any limit point of the sequence $\{x_k\}$ generated by Algorithm 1*

is a stationary point. If moreover the function $H_{\mathcal{N}}$ is convex and the sequence $\{S_k\} \subset \mathcal{M}_\mu$ satisfies the following additional assumption

$$S_{k+1} \preceq (1+\vartheta_k)S_k, \quad \{\vartheta_k\} \subset \mathbb{R}_+, \quad \sum_{k=0}^{+\infty} \vartheta_k < +\infty, \tag{18}$$

then the sequence $\{x_k\}$ converges to a solution of (1).

Proof If there exists $\bar{k}$ such that $N_k \geq N$, $\forall k \geq \bar{k}$, then Algorithm 1 reduces to a deterministic variable metric forward-backward method, whose convergence results are well-known in the literature. The reader is referred for example to [12, Theorem 3.1] and [12, Theorem 3.3]. □

Condition (18) states that the sequence $\{S_k\}_{k\in\mathbb{N}}$ asymptotically approaches a constant matrix [14, Lemma 2.3]. A possibility to practically fulfill this condition (see [12]) is to impose that

$$\{S_k\} \subseteq \mathcal{M}_{\mu_k}, \quad \text{where} \quad \mu_k^2 = 1+\xi_k, \quad \{\xi_k\} \subset \mathbb{R}_+, \quad \sum_{k=0}^{+\infty} \xi_k < +\infty. \tag{19}$$

2.3 Possible practical strategies to select α_k and S_k

A possibility to select the learning rate α_k consists in following the idea suggested in [37]. In particular the Barzilai-Borwein (BB) rules can be adopted in all those iterations where the mini-batch does not change. In this way such rules are employed to efficiently minimize the approximation $H_{\mathcal{N}_k}(\cdot)$ of the objective function. In more detail, let us consider the scenario where the same mini-batch, $\mathcal{N}_k$, is held constant for $m \leq m(\mathcal{N}_k)$ iterations, specifically from iteration k to $k+m-1$. In this case, the learning rate α_j, for $j = k+1, \ldots, k+m-2$, can be chosen using one of the following BB selection rules, which account for the presence of a scaling matrix S_j^{-1} multiplying $\nabla f_{\mathcal{N}_k}(x_j)$:

$$\begin{aligned} \alpha_j^{BB1} &= \frac{z_{j-1}^T S_j z_{j-1}}{z_{j-1}^T y_{j-1}}, \\ \alpha_j^{BB2} &= \frac{z_{j-1}^T y_{j-1}}{y_{j-1}^T S_j^{-1} y_{j-1}}, \end{aligned} \tag{20}$$

where $z_{j-1} = x_j - x_{j-1}$ and $y_{j-1} = \nabla f_{\mathcal{N}_k}(x_j) - \nabla f_{\mathcal{N}_k}(x_{j-1})$. It is evident that, to compute the BB rules, two successive gradients related to the same mini-batch $\mathcal{N}_k$ are required. For this reason, when $j = k$, the learning rate α_j must be set equal to a different predefined value, such as

$$\alpha_j = \frac{1}{\|\nabla f_{\mathcal{N}_k}(x_j)\|}. \tag{21}$$

In the deterministic setting, many variants of the BB rules defined in (20) have been developed to make optimization gradient algorithms more effective. We recall here the so called ABB_{min} strategy [41] which is based on properly alternating the standard BB rules in (20); particularly, for $j = k+1, \ldots, m$, we get

$$\alpha_j^{ABB_{min}} = \begin{cases} \min\{\alpha_i^{BB2} \,|\, i = \max(1, j - M_\alpha), \ldots, j\} & \text{if} \frac{\alpha_j^{BB2}}{\alpha_j^{BB1}} < \tau \\ \alpha_j^{BB1} & \text{otherwise} \end{cases} \tag{22}$$

where $M_\alpha > 0$ is a prefixed integer constant and $\tau \in (0.5, 1)$. Every time the mini-batch changes, the BB rules can not be applied and the learning rate must be fixed differently. A possibility is to follow a strategy similar to (21). Algorithm 2 summarizes the learning rate selection technique just described. It is thought to be integrated in Step 1 of Algorithm 1.

Algorithm 2 BB-like learning rate selection rule

if $flag > 0$ **then**
  Compute $z_{k-1} = x_k - x_{k-1}$ and $y_{k-1} = \nabla f_{\mathcal{N}_k}(x_k) - \nabla f_{\mathcal{N}_k}(x_{k-1})$.
  Compute α_k by means of (20) or (22).
else
  $\alpha_k = \dfrac{1}{\|\nabla f_{\mathcal{N}_k}(x_k)\|}$
end if
$\alpha_k = \min\left(\max\left(\alpha_{min}, \alpha_k\right), \alpha_{max}\right)$

As for the selection of the variable metric, we borrow the ideas of adaptive stochastic gradient methods such as AdaGrad [42], Adam [43] and AdaBelief [44]. The general update iteration of these algorithms can be written as

$$\begin{aligned} x_{k+1} &= x_k - \alpha_k S_k^{-1} m_k \\ m_k &= \gamma m_{k-1} + (1-\gamma)\nabla f_{\mathcal{N}_k}(x_k) \end{aligned}$$

where α_k is a positive learning rate, S_k is a preconditioning matrix and $\gamma \in [0, 1)$ is a constant momentum parameter. Adaptive gradient methods typically differ in how their preconditioners are constructed and whether or not they include the momentum term. For the selection of an appropriate scaling matrix in Algorithm 1, we can consider the preconditioning matrices used in Adam, AdaBelief and AdaGrad, defined respectively as

$$\text{AdaBelief} \begin{cases} M_k = \beta_1 M_{k-1} + (1-\beta_1)\nabla f_{\mathcal{N}_k}(x_k) \\ g_k = \nabla f_{\mathcal{N}_k}(x_k) - M_k \\ S_k = \left(\frac{\beta_2 S_{k-1} + (1-\beta_2) diag\left(g_k g_k^T\right) + \varepsilon I}{1-\beta_2^k} \right)^{1/2} \end{cases} \tag{23}$$

$$\text{Adam} \left\{ S_k = \left(\frac{\beta S_{k-1} + (1-\beta) diag\left(\nabla f_{\mathcal{N}_k}(x_k) \nabla f_{\mathcal{N}_k}(x_k)^T\right) + \varepsilon I}{1-\beta^{\tilde{k}}} \right)^{1/2} \right. \tag{24}$$

$$\text{AdaGrad} \left\{ S_k = \left(S_{k-1} + diag\left(\nabla f_{\mathcal{N}_k}(x_k) \nabla f_{\mathcal{N}_k}(x_k)^T\right) + \varepsilon I \right)^{1/2} \right. \tag{25}$$

where $S_0 = 0$, $M_0 = 0$, $\beta, \beta_1, \beta_2 \in [0, 1)$, $\tilde{k} = k$, $\varepsilon > 0$ and I is the identity matrix. We remark that all these matrices are diagonal with positive diagonal elements, therefore satisfying the requirement to be symmetric and positive definite as needed by Algorithm 1. However, the convergence of Algorithm 1 is guaranteed if the eigenvalues of S_k lie within a suitable interval $\left[\frac{1}{\mu}, \mu\right]$, with $\mu > 0$. As a consequence, the diagonal elements of the matrices S_k in (24), (23) and (25) must be properly thresholded when employed in Algorithm 1. Since condition (18) is needed for the convergence of Algorithm 1 when the full sample is reached, we derive bounds for the scaling matrices based on (19). In particular, given s_k the diagonal of the matrix S_k defined according to one of the definitions (24)-(25), and a summable sequence $\{\xi_k\}$ of non-negative elements, we could impose that

$$s_k = \min\left(\mu_k, \max\left(s_k, \frac{1}{\mu_k}\right)\right) \tag{26}$$

where $\mu_k^2 = 1 + \xi_k$. Actually, requirement (26) is too restrictive to be forced at every iteration of Algorithm 1. Indeed when the mini-batch changes, the bounds for the diagonal elements of S_k can be widened again. The variable $flag$ in Algorithm 1 accounts for the number of iterations with the same mini-batch and, hence, can be employed to reset the bounds for the scaling matrices. A similar strategy can also be adopted to set $\tilde{k}$ in (23) and (24) in order to strengthen the effect of the scaling matrix when the mini-batch changes. In Algorithm 3, we outline our resulting proposal to select the scaling matrix in Step 1 of Algorithm 1.

Algorithm 3 Scaling matrix selection rule

Define S_k by means of (23) with $\tilde{k} = flag$ or (24) with $\tilde{k} = flag$ or (25).
$\mu_k^2 = 1 + \xi_{flag}$
$\text{diag}(S_k) = \min\left(\mu_k, \max\left(\text{diag}(S_k), \frac{1}{\mu_k}\right)\right)$

3 Numerical experiments

In this section we perform several numerical experiments to evaluate the behaviour of the proposed method. We consider a binary classifications problem on four datasets: *w8a*, *IJCNN* and *RCV1* (downloadable from https://www.csie.ntu.edu.tw/~cjlin/libsvmtools/) and *MNIST* (available at https:

//yann.lecun.com/exdb/mnist/). For the *MNIST* dataset, we adapted it for the binary classification dividing the class in odd and even digits.

dataset	d	#training set (N)	#testing set
MNIST	784	60000	10000
w8a	300	44774	4975
IJCNN	22	49990	91701
RCV1	47236	20242	10000

Table 1: Dataset features.

In Table 1 the features of the considered datasets are summarized. Let assume that $(a_i, b_i), i = 1, ...N$ denotes the pair of the feature vector $a_i \in \mathbb{R}^d$ and the class label $b_i \in \{1, -1\}$ of the $i-$th example. We consider two cases for function $f_{\mathcal{N}}(x)$; in the first case the terms of the finite sum are convex logistic regression (LR) loss functions:

$$f_i(x) = \log\left[1 + e^{-b_i a_i^T x}\right],$$

whereas, in the second case, we take into account a finite sum of non-convex loss functions in 2-layer neural networks (NN):

$$f_i(x) = \left(1 - \frac{1}{1 + e^{-b_i a_i^T x}}\right)^2.$$

The regularization term in the objective function $H_{\mathcal{N}}(x)$ can be of two types:

- the L1 norm, $R(x) = \lambda\|x\|_1$; the proximal operator of $\alpha R(x)$ in the S-norm (with S diagonal and positive definite matrix) is given by

$$\text{prox}_{\alpha R}^S(x) = sign(x) \cdot \max((|x| - \alpha\lambda S\mathbf{1}), 0)$$

  where $\mathbf{1}$ is a column vector of d ones, and the product and the absolute value function are intended component-wise;
- and the squared L2 norm, $R(x) = \frac{\lambda}{2}\|x\|_2^2$. The proximal operator of $\alpha R(x)$ in the S-norm (with S diagonal and positive definite matrix) is given by

$$\text{prox}_{\alpha R}^S(x) = \frac{x}{\mathbf{1} + \alpha\lambda S\mathbf{1}}$$

  where the quotient is intended component-wise.

Consequently, the objective function $H_{\mathcal{N}}(x)$ can take four forms, hereafter denoted as LR-L1, NN-L1, LR-L2 and NN-L2. The regularization parameter is fixed as $\lambda = 10^{-4}$ in all the test problems. For any numerical test, we perform 10 runs, leaving the possibility to the random number generator to vary.

Therefore, the performance measures used to evaluate the obtained results are the averaged values of the following quantities:

- optimality gap $H_{\mathcal{N}}(x_k) - H^*_{\mathcal{N}}$, computed on the training set with respect to the epochs; here, $H^*_{\mathcal{N}}$ is an estimate of the minimum value, obtained by running a gradient iterative methods for a huge number of iterations;
- accuracy computed on the testing set with respect to the epochs;
- increase of the mini-batch size with respect to the iterations.

As a measure of computational complexity, we refer to an epoch. By an epoch, we mean the number of operations equivalent to computing the full gradient of the function $f_{\mathcal{N}}(x)$.
In all the experiments, we set the following parameters: $C_{max} = 10^8$, $c_{min} = 10^{-4}$, $\eta = 0.4$, $\beta = 0.5$, $\zeta_0 = 1$; the initial mini-batch size $N_0 = 10$, except when S_k is fixed to the identity matrix, in which case $N_0 = 1$; $\alpha_{min} = 10^{-8}$, $\alpha_{max} = 10^2$, $\bar{\alpha} = 1$ and $m(N_k) = N_k$. The mini-batch size N_k increases according to the rule $N_{k+1} = N_k + 1$.

3.1 L1-regularized test problems

In this subsection, we present the results obtained by the proposed algorithm for the test-problems LR-L1 and NN-L1. The stopping criterion is that the total number of loss term evaluations is greater than or equal to $N \cdot maxit$, where $maxit$ is the maximum number of allowed epochs, set to 20. We also report the execution times for each method to highlight the effectiveness of the new proposed method.

3.1.1 Hyperparameters settings comparison for Algorithm 1

The first numerical experiment compares different versions of the **Prox-SAM** method by varying the selection of either the learning rate α_k or the scaling matrix S_k. In particular we consider the following schemes:

- **Prox-SAM-BB**: Algorithm 1 with S_k equal to the identity matrix and α_k defined by Algorithm 2 equipped by (22);
- **Prox-SAM-I**: Algorithm 1 with S_k equal to the identity matrix and $\alpha_k = 1, \forall k$;
- **Prox-SAM-$S_k^{(1)}$**: Algorithm 1 with S_k selected by Algorithm 3 equipped by (23), $\beta_1 = 0.9$, $\beta_2 = 0.999$, $\varepsilon = 10^{-16}$ and $\alpha_k = 0.5$, $\forall k$;
- **Prox-SAM-$S_k^{(2)}$**: Algorithm 1 with S_k selected by Algorithm 3 equipped by (24), $\beta = 0.999$, $\varepsilon = 10^{-16}$ and $\alpha_k = 0.5, \forall k$;
- **Prox-SAM-$S_k^{(3)}$**: Algorithm 1 with S_k selected by Algorithm 3 equipped by (25), $\varepsilon = 10^{-16}$ and $\alpha_k = 0.5, \forall k$.

For all the scaled versions of **Prox-SAM** the sequence $\{\xi_i\}$ has been chosen as $\left\{\frac{10^5}{(i+1)^{2.1}}\right\}$.

Method		*MNIST*	*w8a*	*IJCNN*	*RCV1*
Prox-SAM-BB	$\lvert H_{\mathcal{N}}(\bar{x}) - H^*_{\mathcal{N}}\rvert$ $\pm STD$	0.0436 $\pm$0.0150	0.0310 $\pm$0.0018	0.0097 $\pm$0.0025	0.0789 $\pm$0.0008
	$A(\bar{x})$ $\pm STD$	0.8863 $\pm$0.0073	0.9428 $\pm$0.0020	0.9197 $\pm$0.0022	0.9417 $\pm$0.0013
	Time (s)	15.3602	5.3616	1.9598	7.4594
Prox-SAM-I	$\lvert H_{\mathcal{N}}(\bar{x}) - H^*_{\mathcal{N}}\rvert$ $\pm STD$	0.1061 $\pm$0.0080	0.0373 $\pm$0.0008	0.0097 $\pm$0.0006	0.1469 $\pm$0.0010
	$A(\bar{x})$ $\pm STD$	0.8867 $\pm$0.0016	0.8996 $\pm$0.0007	0.9155 $\pm$0.0007	0.9408 $\pm$0.0011
	Time (s)	16.8520	5.3854	1.8808	8.1289
Prox-SAM-$S_k^{(1)}$	$\lvert H_{\mathcal{N}}(\bar{x}) - H^*_{\mathcal{N}}\rvert$ $\pm STD$	0.0211 $\pm$0.0024	0.0323 $\pm$0.0010	0.0065 $\pm$0.0003	0.0914 $\pm$0.0009
	$A(\bar{x})$ $\pm STD$	0.8958 $\pm$0.0026	0.9008 $\pm$0.0010	0.9187 $\pm$0.0007	0.9399 $\pm$0.0013
	Time (s)	17.4981	5.1854	1.8789	8.1504
Prox-SAM-$S_k^{(2)}$	$\lvert H_{\mathcal{N}}(\bar{x}) - H^*_{\mathcal{N}}\rvert$ $\pm STD$	0.0213 $\pm$0.0030	0.0323 $\pm$0.0008	0.0065 $\pm$0.0002	0.0914 $\pm$0.0011
	$A(\bar{x})$ $\pm STD$	0.8957 $\pm$0.0017	0.9017 $\pm$0.0012	0.9182 $\pm$0.0009	0.9393 $\pm$0.0013
	Time (s)	17.3483	5.5095	1.8977	8.1797
Prox-SAM-$S_k^{(3)}$	$\lvert H_{\mathcal{N}}(\bar{x}) - H^*_{\mathcal{N}}\rvert$ $\pm STD$	0.0210 $\pm$0.0017	0.0337 $\pm$0.0009	0.0069 $\pm$0.0003	0.0885 $\pm$0.0013
	$A(\bar{x})$ $\pm STD$	0.8969 $\pm$0.0011	0.9011 $\pm$0.0013	0.9184 $\pm$0.0015	0.9395 $\pm$0.0010
	Time (s)	17.3684	5.4844	1.8960	8.5801

Table 2: Results obtained for the test problem LR-L1 with different versions of **Prox-SAM**.

Tables 2-3 report the averaged optimality gap, averaged accuracy with the related standard deviations (STD) and averaged execution time (in seconds) over 10 runs for the LR-L1 and NN-L1 test problems, respectively. From these results we can conclude that, in general, the **Prox-SAM** algorithm with

Method		*MNIST*	*w8a*	*IJCNN*	*RCV1*
Prox-SAM-BB	$\lvert H_{\mathcal{N}}(\bar{x}) - H^*_{\mathcal{N}}\rvert$ $\pm STD$	0.0165 $\pm$0.0024	0.0126 $\pm$0.0004	0.0068 $\pm$0.0010	0.0323 $\pm$0.0002
	$A(\bar{x})$ $\pm STD$	0.8947 $\pm$0.0041	0.8973 $\pm$0.0011	0.9252 $\pm$0.0023	0.9282 $\pm$0.0007
	Time (s)	17.2520	5.9228	2.3742	7.2337
Prox-SAM-I	$\lvert H_{\mathcal{N}}(\bar{x}) - H^*_{\mathcal{N}}\rvert$ $\pm STD$	0.0161 $\pm$0.0009	0.0134 $\pm$0.0003	0.0103 $\pm$0.0004	0.0582 $\pm$0.0003
	$A(\bar{x})$ $\pm STD$	0.8961 $\pm$0.0015	0.8971 $\pm$0.0011	0.9134 $\pm$0.0008	0.9330 $\pm$0.0019
	Time (s)	19.1178	5.9097	2.2695	7.6604
Prox-SAM-$S_k^{(1)}$	$\lvert H_{\mathcal{N}}(\bar{x}) - H^*_{\mathcal{N}}\rvert$ $\pm STD$	0.0120 $\pm$0.0011	0.0137 $\pm$0.0002	0.0061 $\pm$0.0002	0.0366 $\pm$0.0005
	$A(\bar{x})$ $\pm STD$	0.8981 $\pm$0.0025	0.8952 $\pm$0.0013	0.9252 $\pm$0.0012	0.9290 $\pm$0.0016
	Time (s)	18.7752	6.1570	2.2971	7.9079
Prox-SAM-$S_k^{(2)}$	$\lvert H_{\mathcal{N}}(\bar{x}) - H^*_{\mathcal{N}}\rvert$ $\pm STD$	0.0123 $\pm$0.0013	0.0137 $\pm$0.0004	0.0061 $\pm$0.0002	0.0357 $\pm$0.0003
	$A(\bar{x})$ $\pm STD$	0.8983 $\pm$0.0023	0.8950 $\pm$0.0010	0.9239 $\pm$0.0013	0.9295 $\pm$0.0009
	Time (s)	18.5366	6.1225	2.2836	7.9886
Prox-SAM-$S_k^{(3)}$	$\lvert H_{\mathcal{N}}(\bar{x}) - H^*_{\mathcal{N}}\rvert$ $\pm STD$	0.0112 $\pm$0.0005	0.0143 $\pm$0.0004	0.0062 $\pm$0.0003	0.0386 $\pm$0.0005
	$A(\bar{x})$ $\pm STD$	0.9001 $\pm$0.0013	0.8946 $\pm$0.0016	0.9239 $\pm$0.0020	0.9287 $\pm$0.0018
	Time (s)	19.0045	6.1412	2.2905	8.3103

Table 3: Results obtained for the test problem NN-L1 with different versions of **Prox-SAM**.

non-trivial scaling matrices exhibits the best effectiveness. In terms of numerical performance, the least effective version of **Prox-SAM** is **Prox-SAM-I**. Indeed, between the two non-scaled versions of **Prox-SAM**, the one combined with the BB-like rules is more efficient. The final accuracy reached by all the variants of **Prox-SAM** is comparable.

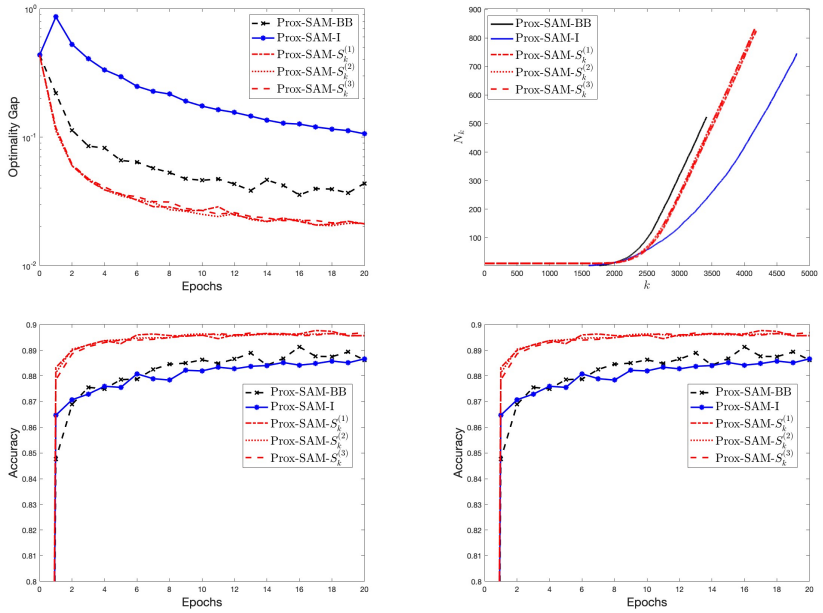

Fig. 1: Test problem LR-L1 for the *MNIST* dataset - First row: averaged optimality gap computed on the training set (left panel) and increase of the averaged mini-batch size (right panel). Second row: averaged accuracy evaluated on the test set (left panel) and a zoom of the accuracy in the interval $[0.8, 0.9]$ (right panel).

Figures 1-2 show the behaviour of the averaged optimality gap, the averaged accuracy and the increase of the averaged mini-batch size over 20 epochs. We can observe that, for the dataset *MNIST* and both the test problems, the configuration **Prox-SAM-**$S_k^{(3)}$ appears very efficient. The accuracy is quite similar across all configurations, and the increase in mini-batch size is limited for all settings, even in relation to the size of the training set. Figures 3-4 show the comparison for the *IJCNN* dataset and the two test problems LR-L1 and NN-L1, respectively. We observe that the use of the scaling techniques is efficient also in this case. In the following comparison with other state-of-the-art algorithms, the **Prox-SAM-**$S_k^{(3)}$ version of the proposed method is adopted.

3.1.2 Comparison of Prox-SAM-$S_k^{(3)}$ with other methods

As in the previous experiment, we perform 10 runs and report the averaged results. We compare the **Prox-SAM-**$S_k^{(3)}$ method with **Prox-SARAH** [28], **Prox-Spider-boost** [45] and **Prox-LISA** [22] equipped with the hyperparameters setting specified in the cited papers. For the sake of completeness, we report these values in Appendix B. We remark that **Prox-SARAH** and **Prox-Spider-boost** are schemes based on outer-inner iterations. At each

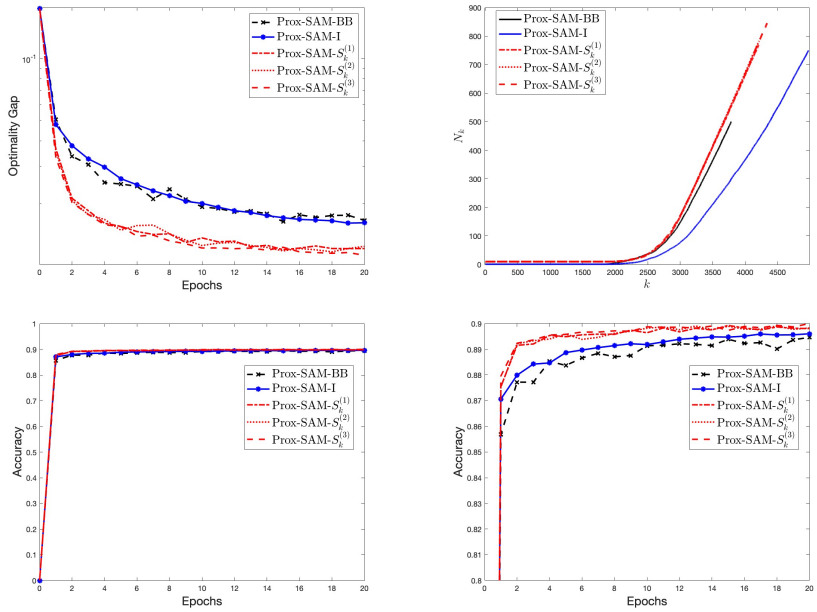

Fig. 2: Test problem NN-L1 for the *MNIST* dataset - First row: averaged optimality gap computed on the training set (left panel) and increase of the average of the mini-batch size (right panel). Second row: averaged accuracy evaluated on the test set (left panel) and a zoom of the accuracy in the interval $[0.8, 0.9]$ (right panel).

outer iteration, the full gradient at the current iterate (or an estimate based on a large mini-batch) is computed and used to evaluate the stochastic gradients in the m successive inner steps, where m is on the order of N. Our implementation of these methods is based on the codes available for download at https://github.com/unc-optimization/StochasticProximalMethods. Here, at each outer iteration the computation of the full gradient is performed.
On the other hand, the **Prox-LISA** algorithm is a stochastic gradient method that uses a line search technique to select the learning rate and performs a test to control the stochastic gradient variance by suitably increasing the mini-batch size.

In Tables 4 and 5 we report the averaged optimality gap, the averaged accuracy obtained by the considered methods for the two test problems LR-L1 and NN-L1, respectively. We also include the averaged execution time in seconds. We observe that the proposed method achieves comparable results to those of **Prox-SARAH** and **Prox-Spider-boost** in a significantly lower computational time. Indeed, **Prox-SARAH** and **Prox-Spider-boost** methods require the very expensive computation of a full gradient at each outer

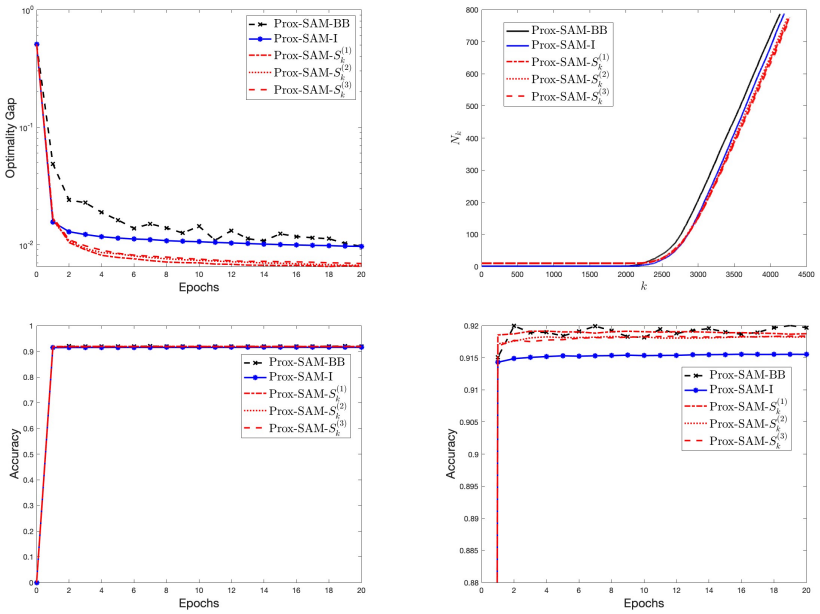

Fig. 3: Test problem LR-L1 for the *IJCNN* dataset - First row: averaged optimality gap computed on the training set (left panel) and increase of the averaged mini-batch size (right panel). Second row: averaged accuracy evaluated on the test set (left panel) and a zoom of the accuracy in the interval $[0.88, 0.92]$ (right panel).

iteration. Compared to the **Prox-LISA** method, the behaviour of **Prox-SAM-**$S_k^{(3)}$ appears very similar. We can conclude that, given the same time budget, **Prox-SARAH** and **Prox-Spider-boost** are not as effective as **Prox-SAM-**$S_k^{(3)}$ and **Prox-LISA**.

In Figure 5 the optimality gap, the accuracy and the increase of the mini-batch size related to the test problem LR-L1 combined with the *RCV1* dataset are shown. In the plot of the optimality gap, the STD is represented by the shaded area around the curves. We observe that, in terms of the optimality gap, the behavior of the considered methods is similar at the end. The final accuracy values for the competitors are slightly higher than those obtained by **Prox-SAM-**$S_k^{(3)}$. However, Figure 7, which reports the optimality gap with respect to the execution time related to one trial, suggests that **Prox-SAM-**$S_k^{(3)}$ and **Prox-LISA** are more efficient in the initial stages of processing. For this type of graph, the different methods are stopped after a time at least equal to the bigger execution time of the pair method/dataset reported in the Tables 4 and 5. The increase in mini-batch size is greater for **Prox-SAM-**$S_k^{(3)}$ than for **Prox-LISA**, but it remains limited relative to the size of the training set. In Figure 6 the optimality gap, the accuracy and the increase of the mini-batch

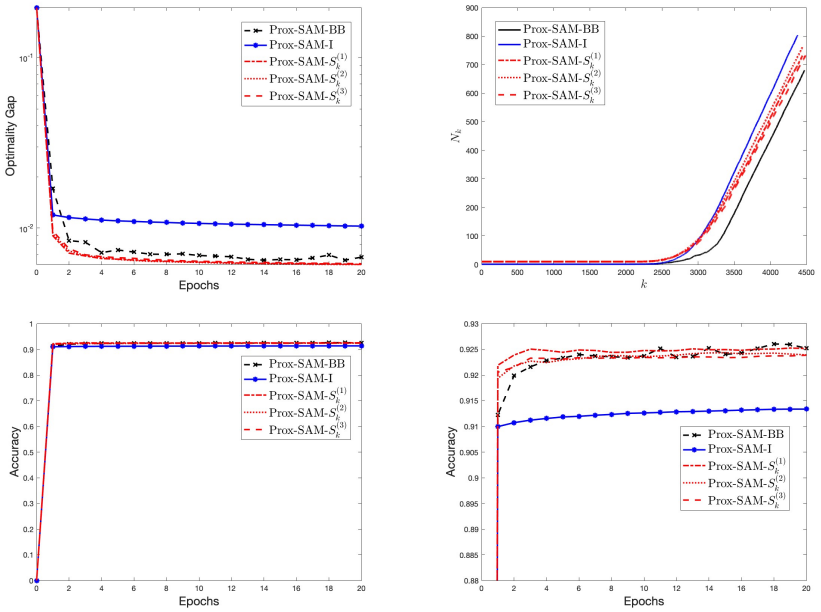

Fig. 4: Test problem NN-L1 for the *IJCNN* dataset - First row: averaged optimality gap computed on the training set (left panel) andincrease of the average of the mini-batch size (right panel). Second row: averaged accuracy evaluated on the test set (left panel) and a zoom of the accuracy in the interval $[0.88, 0.93]$ (right panel).

size are shown for the NN-L1 objective function combined with the *IJCNN* dataset. We observe that the **Prox-SARAH** and **Prox-Spider-boost** methods have a larger STD compared to the other two methods. Furthermore, **Prox-SAM-**$S_k^{(3)}$ exhibits better accuracy than the other methods, even with a lower execution time (see Figure 7).

Method		*MNIST*	*w8a*	*IJCNN*	*RCV1*
Prox-SAM-$S_k^{(3)}$					
	$\lvert H_{\mathcal{N}}(\bar{x}) - H^*_{\mathcal{N}}\rvert$	0.0210	0.0337	0.0069	0.0885
	$\pm STD$	$\pm$0.0017	$\pm$0.0009	$\pm$0.0003	$\pm$0.0013
	$A(\bar{x})$	0.8969	0.9011	0.9184	0.9395
	$\pm STD$	$\pm$0.0011	$\pm$0.0013	$\pm$0.0015	$\pm$0.0010
	Time (s)	17.3684	5.4844	1.8960	8.5801
Prox-SARAH					
	$\lvert H_{\mathcal{N}}(\bar{x}) - H^*_{\mathcal{N}}\rvert$	0.0205	0.0457	0.0085	0.0891
	$\pm STD$	$\pm$0.0002	$\pm$0.0029	$\pm$ 9.74e^{-5}	$\pm$ 6.96e^{-5}
	$A(\bar{x})$	0.8960	0.8964	0.9156	0.9463
	$\pm STD$	$\pm$0.0006	$\pm$0.0010	$\pm$ 8.49e^{-5}	$\pm$0.0005
	Time (s)	30.7269	12.4376	11.0571	91.3117
Prox-Spider-boost					
	$\lvert H_{\mathcal{N}}(\bar{x}) - H^*_{\mathcal{N}}\rvert$	0.0204	0.0853	0.0085	0.0880
	$\pm STD$	$\pm$0.0002	$\pm$0.0002	$\pm$ 9.76e^{-5}	$\pm$ 7.39e^{-5}
	$A(\bar{x})$	0.8961	0.8942	0.9157	0.9465
	$\pm STD$	$\pm$0.0007	$\pm$0.0003	$\pm$ 7.15e^{-5}	$\pm$0.0005
	Time (s)	28.5358	3.7857	11.4335	81.9897
Prox-LISA					
	$\lvert H_{\mathcal{N}}(\bar{x}) - H^*_{\mathcal{N}}\rvert$	0.0173	0.0267	0.0059	0.0950
	$\pm STD$	$\pm$0.0034	$\pm$0.0002	$\pm$ 1.83e^{-6}	$\pm$0.0003
	$A(\bar{x})$	0.8964	0.9032	0.9188	0.9452
	$\pm STD$	$\pm$0.0019	$\pm$0.0005	$\pm$0.0002	$\pm$0.0009
	Time (s)	13.1078	4.3027	2.6623	15.1850

Table 4: Results for LR-L1 test problem after 20 epochs.

Method		*MNIST*	*w8a*	*IJCNN*	*RCV1*
Prox-SAM-$S_k^{(3)}$					
	$\lvert H_{\mathcal{N}}(\bar{x}) - H_{\mathcal{N}}^*\rvert$ $\pm STD$	0.0112 $\pm$0.0005	0.0143 $\pm$0.0004	0.0062 $\pm$0.0003	0.0386 $\pm$0.0005
	$A(\bar{x})$ $\pm STD$	0.9001 $\pm$0.0013	0.8946 $\pm$0.0016	0.9239 $\pm$0.0020	0.9287 $\pm$0.0018
	Time (s)	19.0045	6.1412	2.2905	8.3103
Prox-SARAH					
	$\lvert H_{\mathcal{N}}(\bar{x}) - H_{\mathcal{N}}^*\rvert$ $\pm STD$	0.0137 $\pm$0.0001	0.0153 $\pm$0.0005	0.0340 $\pm$0.0161	0.0302 $\pm$ 2.78e^{-5}
	$A(\bar{x})$ $\pm STD$ Time (s)	0.8951 $\pm$0.0005 28.3576	0.8953 $\pm$0.0004 12.8179	0.9168 $\pm$0.0086 11.4600	0.9324 $\pm$0.0005 89.2021
Prox-Spider-boost					
	$\lvert H_{\mathcal{N}}(\bar{x}) - H_{\mathcal{N}}^*\rvert$ $\pm STD$	0.0228 $\pm$ 4.58e^{-5}	0.0303 $\pm$ 5.19e^{-5}	0.0343 $\pm$0.0162	0.0302 $\pm$ 2.77e^{-5}
	$A(\bar{x})$ $\pm STD$ Time (s)	0.8777 $\pm$0.0003 14.3127	0.8938 $\pm$0.0001 4.0102	0.9168 $\pm$0.0087 11.4218	0.9324 $\pm$0.0004 89.8600
Prox-LISA					
	$\lvert H_{\mathcal{N}}(\bar{x}) - H_{\mathcal{N}}^*\rvert$ $\pm STD$	0.0103 $\pm$0.0002	0.0119 $\pm$ 5.91e^{-5}	0.0063 $\pm$ 3.37e^{-5}	0.0387 $\pm$ 6.50e^{-5}
	$A(\bar{x})$ $\pm STD$ Time (s)	0.8996 $\pm$0.0012 14.7175	0.9002 $\pm$0.0007 4.8300	0.9199 $\pm$0.0002 3.1527	0.9360 $\pm$0.0005 14.5289

Table 5: Results for NN-L1 test problem after 20 epochs.

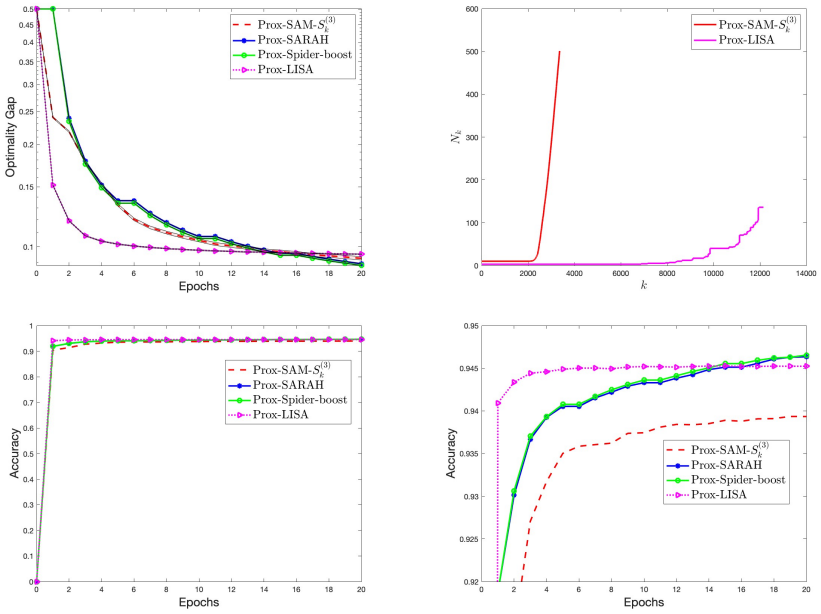

Fig. 5: Test problem LR-L1 for the *RCV1* dataset - First row: averaged optimality gap computed on the training set (left panel) and increase of the averaged mini-batch size (right panel). Second row: averaged accuracy evaluated on the test set (left panel) anda zoom of the accuracy in the interval $[0.92, 0.95]$ (right panel).

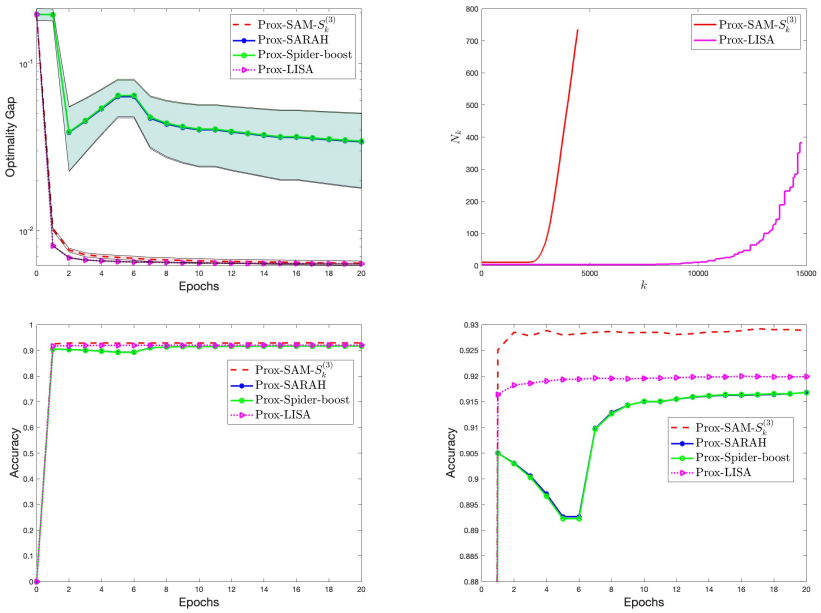

Fig. 6: Test problem NN-L1 for the *IJCNN* dataset - First row: averaged optimality gap computed on the training set (left panel) and increase of the averaged mini-batch size (right panel). Second row: averaged accuracy evaluated on the test set (left panel) and a zoom of the accuracy in the interval $[0.88, 0.93]$ (right panel).

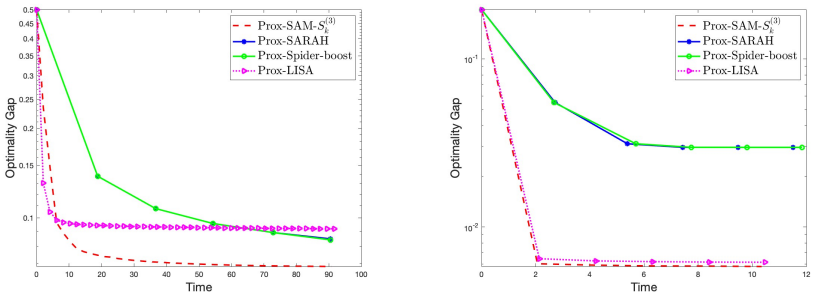

Fig. 7: Optimality gap with respect to the execution time related to one trial for test problem LR-L1 with *RCV1* dataset (left panel) and test problem NN-L1 with *IJCNN* dataset (right panel).

3.2 L2-regularized test problems

In this section we present the results obtained by the proposed method when the regularization term is equal to $\frac{\lambda}{2}\|x\|_2^2$. In particular, the first experiment compares the last four versions of **Prox-SAM** introduced in Section 3.1 with the **LSNM-BB** algorithm [37]. We remark that Prox-SAM exploits the closed form of the proximal operator related to the squared L2 norm, while **LSNM-BB** computes its gradient directly. The methods are stopped when the total number of the loss term evaluations is greater than or equal to $N \cdot maxit$ where $maxit$ is the maximum number of allowed epochs, set equal to 20.

In Tables 6 and 7 we report the averaged optimality gap and the averaged accuracy obtained by the **LSNM-BB** algorithm and the different versions of **Prox-SAM** for the two test problems LR-L2 and NN-L2, respectively. We observe that the scaled versions of the proposed method are very efficient in terms of all metrics compared to **LSNM-BB**.

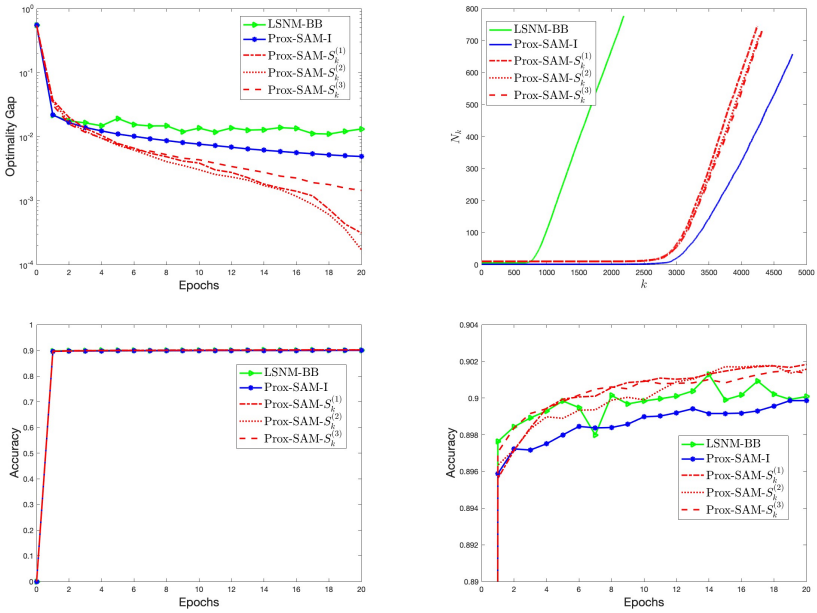

Fig. 8: LR-L2 test problem for the *w8a* dataset - First row: averaged optimality gap computed on the training set (left panel) and increase of the averaged mini-batch size (right panel). Second row: averaged accuracy evaluated on the test set (left panel) and a zoom of the accuracy in the interval $[0.89, 0.904]$ (right panel).

In Figure 8 the optimality gap, the averaged accuracy and the increase of the mini-batch size for the test problem LR-L2 with the *w8a* dataset are shown. We can observe that the three scaled versions of **Prox-SAM** (S_k different to

Method		*MNIST*	*w8a*	*IJCNN*	*RCV1*
LSNM-BB					
	$\lvert H_{\mathcal{N}}(\bar{x}) - H^*_{\mathcal{N}}\rvert$ $\pm STD$	0.0220 $\pm$0.0151	0.0131 $\pm$0.0032	0.0197 $\pm$0.0029	0.0944 $\pm$0.0092
	$A(\bar{x})$ $\pm STD$	0.8895 $\pm$0.0075	0.9001 $\pm$0.0018	0.9134 $\pm$0.0025	0.9459 $\pm$0.0045
	Time (s)	17.8832	5.3414	1.6005	5.0697
Prox-SAM-I					
	$\lvert H_{\mathcal{N}}(\bar{x}) - H^*_{\mathcal{N}}\rvert$ $\pm STD$	0.0641 $\pm$0.0057	0.0049 $\pm$0.0009	0.0014 $\pm$0.0005	0.0322 $\pm$0.0005
	$A(\bar{x})$ $\pm STD$	0.8879 $\pm$0.0021	0.8999 $\pm$0.0013	0.9153 $\pm$0.0009	0.9442 $\pm$0.0013
	Time (s)	16.2417	5.0677	1.8440	7.3271
Prox-SAM-$S_k^{(1)}$					
	$\lvert H_{\mathcal{N}}(\bar{x}) - H^*_{\mathcal{N}}\rvert$ $\pm STD$	0.0064 $\pm$0.0036	0.0003 $\pm$0.0005	0.0003 $\pm$0.0001	0.0063 $\pm$0.0006
	$A(\bar{x})$ $\pm STD$	0.8956 $\pm$0.0020	0.9018 $\pm$0.0007	0.9164 $\pm$0.0005	0.9557 $\pm$0.0007
	Time (s)	17.1458	5.0965	1.8483	7.5063
Prox-SAM-$S_k^{(2)}$					
	$\lvert H_{\mathcal{N}}(\bar{x}) - H^*_{\mathcal{N}}\rvert$ $\pm STD$	0.0069 $\pm$0.0039	0.0002 $\pm$0.0003	0.0003 $\pm$0.0002	0.0065 $\pm$0.0006
	$A(\bar{x})$ $\pm STD$	0.8958 $\pm$0.0029	0.9016 $\pm$0.0015	0.9164 $\pm$0.0006	0.9559 $\pm$0.0006
	Time (s)	16.4497	5.1223	1.8529	7.5341
Prox-SAM-$S_k^{(3)}$					
	$\lvert H_{\mathcal{N}}(\bar{x}) - H^*_{\mathcal{N}}\rvert$ $\pm STD$	0.0046 $\pm$0.0013	0.0014 $\pm$0.0015	0.0004 $\pm$0.0002	0.0080 $\pm$0.0012
	$A(\bar{x})$ $\pm STD$	0.8974 $\pm$0.0012	0.9013 $\pm$0.0009	0.9167 $\pm$0.0005	0.9546 $\pm$0.0014
	Time (s)	16.4121	5.1905	1.8396	7.5470

Table 6: Results obtained for the test problem LR-L2 with different versions of **Prox-SAM**.

the identity matrix) are very efficient. The increase of the mini-batch size is very similar for all the considered versions of **Prox-SAM**. The final accuracy is around 0.9 in all cases. In Figure 9 the optimality gap, the accuracy and the increase of the mini-batch size for the NN-L2 objective function combined

Method		*MNIST*	*w8a*	*IJCNN*	*RCV1*
LSNM-BB	$\lvert H_{\mathcal{N}}(\bar{x}) - H^*_{\mathcal{N}}\rvert$ $\pm STD$	0.0079 $\pm$0.0046	0.0044 $\pm$0.0005	0.0074 $\pm$0.0006	0.0356 $\pm$0.0057
	$A(\bar{x})$ $\pm STD$	0.8912 $\pm$0.0101	0.9012 $\pm$0.0011	0.9117 $\pm$0.0015	0.9428 $\pm$0.0056
	Time (s)	16.9037	5.5032	1.8646	5.3847
Prox-SAM-I	$\lvert H_{\mathcal{N}}(\bar{x}) - H^*_{\mathcal{N}}\rvert$ $\pm STD$	0.0060 $\pm$0.0007	0.0002 $\pm$0.0005	0.0013 $\pm$0.0002	0.0122 $\pm$0.0003
	$A(\bar{x})$ $\pm STD$	0.8963 $\pm$0.0012	0.8976 $\pm$0.0011	0.9117 $\pm$0.0014	0.9409 $\pm$0.0016
	Time (s)	17.5193	5.8471	2.1605	7.1475
Prox-SAM-$S_k^{(1)}$	$\lvert H_{\mathcal{N}}(\bar{x}) - H^*_{\mathcal{N}}\rvert$ $\pm STD$	0.0015 $\pm$0.0005	0.0013 $\pm$0.0005	6.96e^{-5} $\pm$ 5.54e^{-5}	0.0013 $\pm$0.0004
	$A(\bar{x})$ $\pm STD$	0.8998 $\pm$0.0013	0.8985 $\pm$0.0014	0.9164 $\pm$0.0004	0.9544 $\pm$0.0008
	Time (s)	17.6217	5.7809	2.1728	7.4940
Prox-SAM-$S_k^{(2)}$	$\lvert H_{\mathcal{N}}(\bar{x}) - H^*_{\mathcal{N}}\rvert$ $\pm STD$	0.0016 $\pm$0.0005	0.0013 $\pm$0.0005	5.17e^{-5} $\pm$ 4.68e^{-5}	0.0011 $\pm$0.0003
	$A(\bar{x})$ $\pm STD$	0.9000 $\pm$0.0019	0.8991 $\pm$0.0007	0.9164 $\pm$0.0004	0.9542 $\pm$0.0009
	Time (s)	18.1867	5.6715	2.1401	7.4712
Prox-SAM-$S_k^{(3)}$	$\lvert H_{\mathcal{N}}(\bar{x}) - H^*_{\mathcal{N}}\rvert$ $\pm STD$	0.0017 $\pm$0.0004	0.0020 $\pm$0.0004	6.82e^{-5} $\pm$ 5.41e^{-5}	0.0011 $\pm$0.0002
	$A(\bar{x})$ $\pm STD$	0.9003 $\pm$0.0011	0.8983 $\pm$0.0006	0.9167 $\pm$0.0004	0.9537 $\pm$0.0007
	Time (s)	18.5474	5.7919	2.1568	7.5859

Table 7: Results obtained for the test problem NN-L2 with different versions of **Prox-SAM**.

with the *MNIST* dataset are shown. Similar conclusions to those drawn from Figure 8 can also be made in this case.

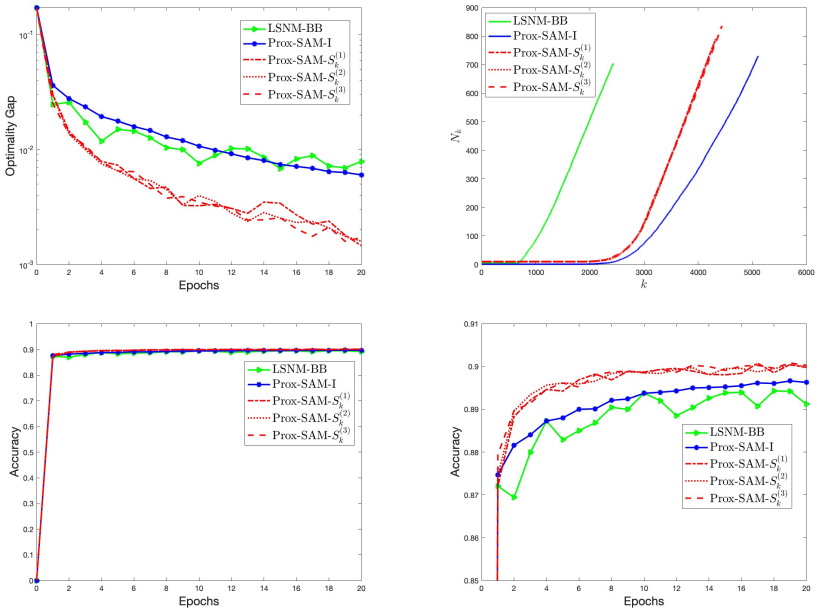

Fig. 9: Test problem NN-L2 for the *MNIST* dataset - First row: averaged optimality gap computed on the training set (left panel) and increase of the averaged mini-batch size (right panel). Second row: averaged accuracy evaluated on the test set (left panel) anda zoom of the accuracy in the interval $[0.85, 0.91]$ (right panel).

3.2.1 Comparison of Prox-SAM-$S_k^{(3)}$ with other methods

As in the previous experiments with the $L1$ regularization term, we compare **Prox-SAM-**$S_k^{(3)}$ with **Prox-SARAH**, **Prox-Spider-boost** and **Prox-LISA**.

In Tables 8 and 9 we report the averaged optimality gap and the averaged accuracy obtained by the considered methods for the two test problems LR-L2 and NN-L2, respectively. We notice that, also in the presence of the L2 regularization term, **Prox-SAM-**$S_k^{(3)}$ appears very efficient compared to **Prox-SARAH** and **Prox-Spider-boost**. We also find that, with respect to the **Prox-LISA** method, the behaviour of **Prox-SAM-**$S_k^{(3)}$ appears equivalent and, for some test problem/dataset combinations, more efficient. It is worth stressing that **Prox-SAM-**$S_k^{(3)}$ and **Prox-LISA** require shorter execution times than **Prox-SARAH** and **Prox-Spider-Boost**.

In Figure 10 the optimality gap, the accuracy and the increase of the mini-batch size for the test problem LR-L2 with the *IJCNN* dataset are shown. We observe that after few epochs, the proposed method becomes more efficient compared to the other methods. The final accuracy is very similar across all

Method		*MNIST*	*w8a*	*IJCNN*	*RCV1*
Prox-SAM-$S_k^{(3)}$	$\lvert H_{\mathcal{N}}(\bar{x}) - H_{\mathcal{N}}^*\rvert$ $\pm STD$	0.0046 $\pm$0.0013	0.0014 $\pm$0.0014	0.0004 $\pm$ 0.0002	0.0080 $\pm$0.0012
	$A(\bar{x})$ $\pm STD$ Time (s)	0.8974 $\pm$0.0012 16.4121	0.9013 $\pm$0.0009 5.1905	0.9167 $\pm$0.0005 1.8396	0.9546 $\pm$0.0014 7.5470
Prox-SARAH	$\lvert H_{\mathcal{N}}(\bar{x}) - H_{\mathcal{N}}^*\rvert$ $\pm STD$	0.0061 $\pm$0.0003	0.0126 $\pm$0.0020	0.0024 $\pm$ 4.36e^{-5}	0.0158 $\pm$ 5.79e^{-6}
	$A(\bar{x})$ $\pm STD$ Time (s)	0.8965 $\pm$0.0006 28.4986	0.8966 $\pm$0.0010 13.2941	0.9147 $\pm$ 8.10e^{-5} 11.0751	0.9539 $\pm$0.0002 83.0225
Prox-Spider-boost	$\lvert H_{\mathcal{N}}(\bar{x}) - H_{\mathcal{N}}^*\rvert$ $\pm STD$	0.0060 $\pm$0.0003	0.0577 $\pm$0.0002	0.0024 $\pm$ 4.34e^{-5}	0.0157 $\pm$ 5.43e^{-6}
	$A(\bar{x})$ $\pm STD$ Time (s)	0.8965 $\pm$0.0006 31.7880	0.8945 $\pm$0.0005 3.9925	0.9147 $\pm$ 9.02e^{-5} 11.2167	0.9539 $\pm$0.0002 77.1612
Prox-LISA	$\lvert H_{\mathcal{N}}(\bar{x}) - H_{\mathcal{N}}^*\rvert$ $\pm STD$	0.0002 $\pm$0.0004	0.0011 $\pm$ 7.79e^{-5}	0.0015 $\pm$ 6.60e^{-5}	0.0165 $\pm$ 7.89e^{-5}
	$A(\bar{x})$ $\pm STD$ Time (s)	0.8981 $\pm$0.0017 13.4784	0.9016 $\pm$0.0005 4.5602	0.9153 0.0002 2.6196	0.9533 $\pm$0.0005 18.4673

Table 8: Results for LR-L2 test problem after 20 epochs.

methods, and although the mini-batch size increase for **Prox-SAM-**$S_k^{(3)}$ is larger than for **Prox-LISA**, it remains smaller than the size of the training set. Similar observations can be made for Figure 11, which shows the optimality gap, accuracy, and mini-batch size increase for the *RCV1* dataset with the NN-L2 objective function. Also in this case, Figure 12, which reports the optimality gap with respect to the execution time related to one trial, suggests that **Prox-SAM-**$S_k^{(3)}$ and **Prox-LISA** are more efficient in the initial stages of processing.

4 Conclusions

In this paper we proposed a class of variable metric proximal stochastic gradient methods aimed at solving regularized empirical risk minimization problems. Besides the presence of a scaling matrix in the stochastic direction, our proposal is based on a line search, monitoring the decrease of the stochastic approximations of the objective function, and an increasing mini-batch size strategy, combined with an additional sampling procedure. Specifically, the mini-batch remains fixed until the additional sampling condition is no longer satisfied or a predefined number of iterations has been reached. We

Method		*MNIST*	*w8a*	*IJCNN*	*RCV1*
Prox-SAM-$S_k^{(3)}$					
	$\lvert H_{\mathcal{N}}(\bar{x}) - H_{\mathcal{N}}^*\rvert$	0.0017	0.0020	6.82e^{-5}	0.0011
	$\pm STD$	$\pm$0.0004	$\pm$0.0004	$\pm$ 5.41e^{-5}	$\pm$0.0002
	$A(\bar{x})$	0.9003	0.8983	0.9167	0.9537
	$\pm STD$	$\pm$0.0011	$\pm$0.0006	$\pm$0.0004	$\pm$0.0007
	Time (s)	18.5474	5.7919	2.1568	7.5859
Prox-SARAH					
	$\lvert H_{\mathcal{N}}(\bar{x}) - H_{\mathcal{N}}^*\rvert$	0.0047	0.0037	0.0010	0.0054
	$\pm STD$	$\pm$ 0.0002	$\pm$0.0004	$\pm$ 9.54e^{-7}	$\pm$ 3.65e^{-7}
	$A(\bar{x})$	0.8957	0.8964	0.9140	0.9519
	$\pm STD$	$\pm$ 0.0007	$\pm$0.0007	$\pm$ 1.49e^{-5}	$\pm$ 5.68e^{-5}
	Time (s)	29.1376	12.9377	11.6434	88.9644
Prox-Spider-boost					
	$\lvert H_{\mathcal{N}}(\bar{x}) - H_{\mathcal{N}}^*\rvert$	0.0161	0.0219	0.0010	0.0054
	$\pm STD$	$\pm$ 5.53e^{-5}	$\pm$ 6.11e^{-5}	$\pm$ 1.06e^{-6}	$\pm$ 4.12e^{-7}
	$A(\bar{x})$	0.8780	0.8948	0.9140	0.9519
	$\pm STD$	$\pm$0.0003	$\pm$0.0004	$\pm$ 1.66e^{-5}	$\pm$ 7.38e^{-5}
	Time (s)	14.6851	4.1203	11.7156	79.0045
Prox-LISA					
	$\lvert H_{\mathcal{N}}(\bar{x}) - H_{\mathcal{N}}^*\rvert$	0.0004	0.0004	0.0010	0.0058
	$\pm STD$	$\pm$ 0.0001	$\pm$ 3.12e^{-5}	$\pm$ 2.10e^{-5}	$\pm$ 2.32e^{-5}
	$A(\bar{x})$	0.9002	0.8995	0.9140	0.9508
	$\pm STD$	$\pm$0.0009	$\pm$ 0.0004	$\pm$ 0.0002	$\pm$0.0007
	Time (s)	14.8462	4.4205	3.3125	19.4039

Table 9: Results for NN-L2 test problem after 20 epochs.

have studied the convergence properties of our proposed scheme for strongly convex, convex, and non-convex functions, notably without requiring Lipschitz continuity of the gradient for the differentiable part of the objective function. Numerical experiments on binary classification tasks validate the effectiveness of our approach, showcasing its promising performance relative to existing state-of-the-art proximal stochastic gradient methods. Future work will focus on extending the approach to more complex tasks, such as multi-class classification and deep learning models.

Acknowledgments

This work was partially supported by "Gruppo Nazionale per il Calcolo Scientifico (GNCS-INdAM)" (Progetti 2024).
F. Porta is partially supported by the the Italian MUR through the PRIN 2022 Project "Numerical Optimization with Adaptive Accuracy and Applications to Machine Learning", project code: 2022N3ZNAX (CUP E53D2300 7700006), under the National Recovery and Resilience Plan (PNRR), Italy, Mission 04 Component 2 Investment 1.1 funded by the European Commission - NextGeneration EU programme.

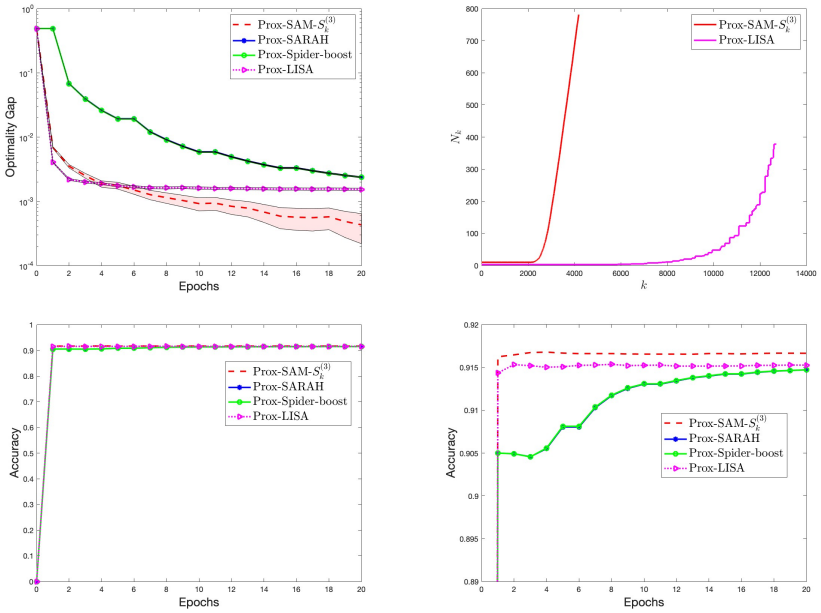

Fig. 10: LR-L2 test problem for the *IJCNN* dataset - First row: averaged optimality gap computed on the training set (left panel) and increase of the averaged mini-batch size (right panel). Second row: averaged accuracy evaluated on the test set (left panel) and a zoom of the accuracy in the interval $[0.89, 0.92]$ (right panel).

F. Porta is partially supported by the the Italian MUR through the PRIN 2022 PNRR Project "Advanced optimization METhods for automated central veIn Sign detection in multiple sclerosis from magneTic resonAnce imaging (AMETISTA)", project code: P2022J9SNP (CUP E53D23017980001), under the National Recovery and Resilience Plan (PNRR), Italy, Mission 04 Component 2 Investment 1.1 funded by the European Commission - NextGeneration EU programme.
V. Ruggiero and I. Trombini were partially funded by European Union - NextGenerationEU through the Italian Ministry of University and Research as part of the PNRR – Mission 4 Component 2, Investment 1.3 (MUR Directorial Decree no. 341 of 03/15/2022), FAIR "Future" Partnership Artificial Intelligence Research", Proposal Code PE00000013 - CUP J33C22002830006).
Krklec Jerinkić is supported by the Science Fund of the Republic of Serbia, Grant no. 7359, Project LASCADO.

Availability of Data and Materials

The datasets analysed during the current study are available in links given in the paper.

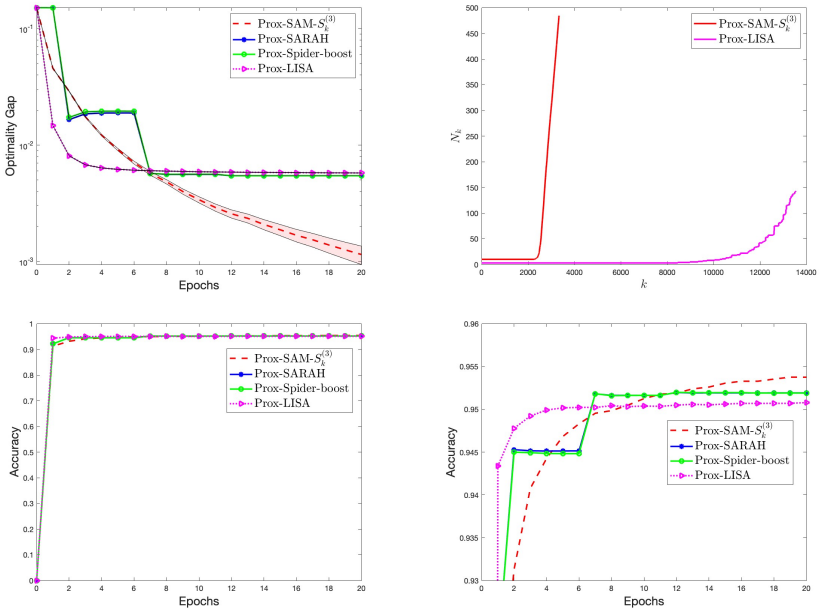

Fig. 11: NN-L2 test problem for the *RCV1* dataset - First row: averaged optimality gap computed on the training set (left panel) and increase of the averaged mini-batch size (right panel)Second row: averaged accuracy evaluated on the test set (left panel) and a zoom of the accuracy in the interval $[0.93, 0.96]$ (right panel).

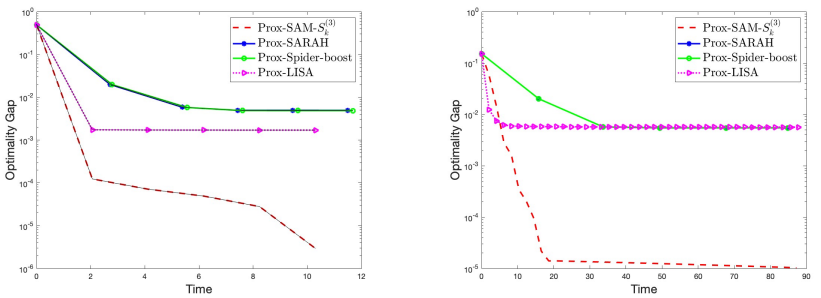

Fig. 12: Optimality gap with respect to the execution time related to one trial for test problem LR-L2 with *RCV1* dataset (left panel) and test problem NN-L2 with *IJCNN* dataset (left panel).

Conflict of interest

The authors have no relevant financial or non-financial interests to disclose.

References

[1] Hastie, T., Tibshirani, R., Friedman, J.: The elements of statistical learning: Data mining, inference, and prediction. Springer New York (2009)

[2] Bottou, L., Curtis, F.E., Nocedal, J.: Optimization methods for large-scale machine learning. SIAM Review **60**(2), 223–311 (2018)

[3] Bottou, L.: Online learning and stochastic approximations. Cambridge University Press, New York, NY, USA, 9–42 (1998)

[4] Goodfellow, I., Bengio, Y., Courville, A.: Deep learning, volume 1. MIT press Cambridge (2016)

[5] Sra, S., Nowozin, S., Wright, S.J.: Optimization for machine learning. Mit Press (2012)

[6] Bertero, M., Boccacci, P.: Introduction to inverse problems in imaging. Institute of Physics, Bristol, England (1998)

[7] Bertero, M., Boccacci, P., Ruggiero, V.: Inverse imaging with poisson data. Institute of Physics, Bristol, England (2018). https://doi.org/10.1088/2053-2563/aae109

[8] Combettes, P.L., Wajs, V.R.: Signal recovery by proximal forward-backward splitting. SIAM Multiscale Model. Simul. **4**, 1168–1200 (2005)

[9] Combettes, P.L., Pesquet, J.-C.: Proximal splitting methods in signal processing. In: Bauschke, H.H., Burachik, R.S., Combettes, P.L., Elser, V., Luke, D.R., Wolkowicz, H. (eds.) Fixed-point Algorithms for Inverse Problems in Science and Engineering. Springer Optimization and Its Applications, pp. 185–212. Springer, ??? (2011)

[10] Attouch, H., Bolte, J., Svaiter, B.F.: Convergence of descent methods for semi–algebraic and tame problems: proximal algorithms, forward–backward splitting, and regularized Gauss–Seidel methods. Math. Program. **137**, 91–129 (2013)

[11] Bonettini, S., Porta, F., Prato, M., Rebegoldi, S., Ruggiero, V., Zanni, L.: Recent advances in variable metric first-order methods. In: M. Donatelli, S.S.-C. (ed.) Computational Methods for Inverse Problems in Imaging vol. 36, pp. 1–31. Springer, ??? (2019)

[12] Bonettini, S., Loris, I., Porta, F., Prato, M.: Variable metric inexact line-search based methods for nonsmooth optimization. SIAM Journal on Optimization **26**, 891–921 (2016)

[13] Chouzenoux, E., Pesquet, J.C., Repetti, A.: Variable metric forward-backward algorithm for minimizing the sum of a differentiable function and a convex function. J. Optim. Theory Appl. **162**, 107–132 (2014)

[14] Combettes, P.L., Vũ, B.: Variable metric quasi-féjer monotonicity. Nonlinear Anal. **78**, 17–31 (2013)

[15] Frankel, P., Garrigos, G., Peypouquet, J.: Splitting methods with variable metric for Kurdyka-Lojasiewicz functions and general convergence rates. J. Optim. Theory Appl. **165**, 874–900 (2015)

[16] Salzo, S.: The variable metric forward-backward splitting algorithm under mild differentiability assumptions. SIAM J. Optim. **27**(4), 2153–2181 (2017)

[17] Khaled, A., Sebbouh, O., Loizou, N., Gower, R.M., Richtárik, P.: Unified analysis of stochastic gradient methods for composite convex and smooth optimization. J. Optim. Theory Appl. **199**, 499–540 (2023)

[18] Duchi, J., Singer, Y.: Efficient online and batch learning using forward backward splitting. J. Mach. Learn. Res. **10**, 2899–2934 (2009)

[19] Bollapragada, R., Byrd, R., Nocedal, J.: Adaptive sampling strategies for stochastic optimization. SIAM Journal on Optimization **28**(4), 3312–3343 (2018)

[20] Richard H Byrd, R.H., Chin, G.M., Nocedal, J., Wu, Y.: Sample size selection in optimization methods for machine learning. Mathematical Programming **134**(1), 127–155 (2012)

[21] Cartis, C., Scheinberg, K.: Global convergence rate analysis of unconstrained optimization methods based on probabilistic models. Mathematical Programming, 1–39 (2015)

[22] Franchini, G., Porta, F., Ruggiero, V., Trombini, I.: A line search based proximal stochastic gradient algorithm with dynamical variance reduction. Journal of Scientific Computing **94**, 23 (2023)

[23] Franchini, G., Porta, F., Ruggiero, V., Trombini, I., Zanni, L.: Learning rate selection in stochastic gradient methods based on line search strategies. Applied Mathematics in Science and Engineering **31**(1), 2164000 (2023)

[24] Friedlander, M.P., Schmidt, M.: Hybrid deterministic-stochastic methods for data fitting. SIAM Journal on Scientific Computing **34**(3), 1380–1405 (2012)

[25] Hashemi, F.H., Ghosh, S., Pasupathy, R.: On adaptive sampling rules for stochastic recursions. Simulation Conference (WSC), 2014 Winter, 3959–3970 (2014)

[26] Poon, C., Liang, J., Schoenlieb, C.: Local convergence properties of SAGA/Prox-SVRG and acceleration. In: Dy, J., Krause, A. (eds.) Proceedings of the 35th International Conference on Machine Learning. Proceedings of Machine Learning Research, vol. 80, pp. 4124–4132 (2018)

[27] Xiao, L., Zhang, T.: A proximal stochastic gradient method with progressive variance reduction. SIAM J. Optim. **24**(4), 2057–2075 (2014)

[28] Phamy, N.H., Nguyen, L.M., Phan, D.T., Tran–Dinh, Q.: Proxsarah: An effcient algorithmic framework for stochastic composite nonconvex optimization. Journal of Machine Learning Research **21**, 1–48 (2020)

[29] Wang, Z., Ji, K., Zhou, Y., Liang, Y., Tarokh, V.: Spiderboost and momentum: Faster stochastic variance reduction algorithms. In: Proceedings of the 33rd International Conference on Neural Information Processing Systems, Curran Associates Inc., vol. 216, pp. 2406–2416 (2019)

[30] Fort, G., Moulines, E.: Stochastic variable metric proximal gradient with variance reduction for non-convex composite optimization. Stat. Comput. **33**, 65 (2023)

[31] Defazio, A., Bach, F., Lacoste-Julien, S.: Saga: A fast incremental gradient method with support for non-strongly convex composite objectives. In: Advances in Neural Information Processing Systems, pp. 1646–1654 (2014)

[32] Johnson, R., Zhang, T.: Accelerating stochastic gradient descent using predictive variance reduction. In: Advances in Neural Information Processing Systems, pp. 315–323 (2013)

[33] Franchini, G., Porta, F., Ruggiero, V., Trombini, I., Zanni, L.: A stochastic gradient method with variance control and variable learning rate for deep learning. Journal of Computational and Applied Mathematics **451**, 116083 (2024)

[34] Paquette, C., Scheinberg, K.: A stochastic line search method with expected complexity analysis. SIAM Journal on Optimization **30**(1), 349–376 (2020)

[35] Vaswani, S., Mishkin, A., Laradji, I., Schmidt, M., Gidel, G., Lacoste-Julien, S.: Painless stochastic gradient; interpolation, line–search, and convergence rates. Advances in Neural Information Processing Systems

32, 3312–3343 (2018)

[36] di Serafino, D., Krejić, N., Jerinkić, N.K., Viola, M.: LSOS: Line-search Second-Order Stochastic optimization methods for nonconvex finite sums (2022)

[37] Krklec Jerinkić, N., Trombini, I., Ruggiero, V.: Spectral stochastic gradient method with additional sampling for finite and infinite sums. submitted (2024)

[38] Bellavia, S., Krejić, N., Jerinkić, N.K., Raydan, M.: SLiSeS: Subsampled Line Search Spectral Gradient Method for Finite Sums (2023)

[39] Krejić, N., Krklec Jerinkić, N., Martínez, A., Yousefi, M.: A non-monotone trust-region method with noisy oracles and additional sampling (2024). https://doi.org/10.48550/arXiv.2307.10038

[40] Polyak, B.T.: Introduction to optimization. Optimization Software (1987)

[41] Frassoldati, G., Zanghirati, G., Zanni, L.: New adaptive stepsize selections in gradient methods. J. Ind. Manag. Optim. **4**(2), 299–312 (2008)

[42] Duchi, J.C., Hazan, E., Singer, Y.: Adaptive subgradient methods for online learning and stochastic optimization. The Journal of Machine Learning Research **12**, 2121–2159 (2011)

[43] Kingma, D.P., Ba, J.: Adam: A method for stochastic optimization. In: 3rd International Conference on Learning Representations, ICLR (2015)

[44] Zhuang, J., Tang, T., Ding, Y., Tatikonda, S.C., Dvornek, N., Papademetris, X., Duncan, J.: Adabelief optimizer: Adapting stepsizes by the belief in observed gradients. Adv. Neural Inf. Process. Syst. **33** (2020)

[45] Wang, Z., Ji, K., Zhou, Y., Liang, Y., Tarokh, V.: SpiderBoost and momentum: faster stochastic variance reduction algorithms. Curran Associates Inc., Red Hook, NY, USA (2019)

A Auxiliary results

A.1 Properties of the proximal operator

Lemma A.1 recalls well known results on the proximal operator (for the proof, see [9, 12] and references therein).

Lemma A.1. *Let $\alpha > 0$, S be a symmetric positive definite matrix, $x \in dom(H_\Sigma)$ with $\Sigma \subseteq \mathcal{N}$. Given the function*

$$q_\Sigma^{\alpha,S}(y) = (y-x)^T \nabla f_\Sigma(x) + \frac{1}{2\alpha}\|y-x\|_S^2 + R(y) - R(x),$$

the following statements hold true.

a. $\hat{y} = \operatorname{prox}_{\alpha R}^S(x - \alpha S^{-1}u)$ *if and only if* $\frac{1}{\alpha}S(x-\hat{y}) - u = w$, $w \in \partial R(\hat{y})$.
b. $q_\Sigma^{\alpha,S}(x) = 0$.
c. *Given* $v^{(\Sigma)} = \operatorname{prox}_{\alpha R}^S(x - \alpha S^{-1}\nabla f_\Sigma(x))$, $q_\Sigma^{\alpha,S}(v^{(\Sigma)}) \leq 0$ *and* $q_\Sigma^{\alpha,S}(v^{(\Sigma)}) = 0$ *if and only if* $v^{(\Sigma)} = x$.
d. x *is a stationary point for problem* $min_{y\in\mathbb{R}^d} f_\Sigma(y) + R(y)$ *if and only if* $x = v^{(\Sigma)}$ *if and only if* $q_\Sigma^{\alpha,S}(v^{(\Sigma)}) = 0$.

A.2 Proof of Lemma 2.1

Assume by contradiction that there exists a $k \in \mathbb{N}$ such that Step 4 in Algorithm 1 performs an infinite number of reductions. As a consequence, for any $j \in \mathbb{N}$ we have

$$\begin{aligned}
\eta q_{\mathcal{N}_k}^{\alpha_k,S_k}(v_k^{(\mathcal{N}_k)}) &< \frac{H_{\mathcal{N}_k}(x_k + \beta^j d_k^{(\mathcal{N}_k)}) - H_{\mathcal{N}_k}(x_k)}{\beta^j} = \\
&= \frac{f_{\mathcal{N}_k}(x_k + \beta^j d_k^{(\mathcal{N}_k)}) - f_{\mathcal{N}_k}(x_k)}{\beta^j} + \frac{R(x_k + \beta^j d_k^{(\mathcal{N}_k)}) - R(x_k)}{\beta^j} \\
&\leq \frac{f_{\mathcal{N}_k}(x_k + \beta^j d_k^{(\mathcal{N}_k)}) - f_{\mathcal{N}_k}(x_k)}{\beta^j} + \\
&\quad + \frac{\beta^j R(x_k + d_k^{(\mathcal{N}_k)}) + (1-\beta^j)R(x_k) - R(x_k)}{\beta^j} \\
&= \frac{f_{\mathcal{N}_k}(x_k + \beta^j d_k^{(\mathcal{N}_k)}) - f_{\mathcal{N}_k}(x_k)}{\beta^j} + R(v_k^{(\mathcal{N}_k)}) - R(x_k),
\end{aligned}$$

where the second inequality follows by applying the convexity of function R. Taking the limit on the right-hand side for $j \to +\infty$, we obtain

$$\begin{aligned}
\eta q_{\mathcal{N}_k}^{\alpha_k,S_k}(v_k^{(\mathcal{N}_k)}) &\leq \nabla f_{\mathcal{N}_k}(x_k)^T d_k^{(\mathcal{N}_k)} + R(v_k^{(\mathcal{N}_k)}) - R(x_k) \\
&\leq \nabla f_{\mathcal{N}_k}(x_k)^T d_k^{(\mathcal{N}_k)} + R(v_k^{(\mathcal{N}_k)}) - R(x_k) + \frac{1}{2\alpha_k}\|v_k^{(\mathcal{N}_k)} - x_k\|_{S_k}^2 \\
&= q_{\mathcal{N}_k}^{\alpha_k,S_k}(v_k^{(\mathcal{N}_k)}).
\end{aligned}$$

Since $0 < \eta < 1$ and the line search is performed only if $q_{\mathcal{N}_k}^{\alpha_k,S_k}(v_k^{(\mathcal{N}_k)})$ is non-zero, this is an absurdum.

A.3 Proof of Lemma 2.2

Assume that $N_k < N$ for all $k \in \mathbb{N}$. Since the sample size sequence $\{N_k\}$ in Algorithm 1 is non-decreasing, this means that there exists some $\overline{N} < N$ and $k_2 \in \mathbb{N}$ such that $N_k = \overline{N}$ for all $k \geq k_2$. Now, let us assume that there is no $k_1 \in \mathbb{N}$ such that $\mathcal{D}_k^- = \emptyset$ for all $k \geq k_1$. This means that there exists an infinite sub-sequence of iterations $K \subseteq \mathbb{N}$ such that $\mathcal{D}_k^- \neq \emptyset$ for all $k \in K$. Since $\mathcal{D}_k$ is chosen randomly and uniformly, with finitely many possible outcomes for each k, there exists some $q > 0$ such that $\mathbb{P}(\mathcal{D}_k \in \mathcal{D}_k^-) \geq q$ for all $k \in K$. So, we have

$$\mathbb{P}(\mathcal{D}_k \in \mathcal{D}_k^+, k \in K) \leq \Pi_{k \in K}(1-q) = 0;$$

this means that we will almost surely encounter an iteration at which the sample size will be increased due to violation of the additional sampling condition in Step 6 of Algorithm 1. This is a contradiction with the sample size being kept to $\overline{N}$ during the whole optimization process. Thus, we conclude that the statement holds.

B Hyperparameter settings for hybrid methods.

For the **Prox-SARAH** method we use the hyperparameter setting specified in [28] where, by borrowing the notation of the referred paper, $q = 2+0.01+(\frac{1}{100})$, $C = \frac{q^2}{(q^2+8)\hat{L}^2\gamma^2}$ and the values for the other hyperparameters are shown in Table 10.

For the **Prox-Spider-boost** method we use the hyperparameter setting specified in [45] and the values for the hyperparameters are shown in Table 11.

Method	Loss	γ	α	$\overline{N}$	m
MNIST	LR	0.99	α_{opt}	1	2N
MNIST	NN	0.99	$\frac{0.1}{\hat{L}}$	1	2N
w8a	LR	0.99	$\frac{0.1}{\hat{L}}$	1	2N
w8a	NN	0.99	$\frac{0.1}{\hat{L}}$	1	2N
IJCNN	LR	0.99	α_{opt}	1	2N
IJCNN	NN	0.99	α_{opt}	1	2N
RCV1	LR	0.95	α_{opt}	1	2N
RCV1	NN	0.95	α_{opt}	1	2N

Table 10: Settings for Prox-SARAH [28].

α_{opt} is the best tuned value obtained after a time and resource consuming procedure of repeated trials. This setting is the same for both the regularization terms.

In the implementation of **Prox-LISA** method, the initial mini batch size is $N_0 = 3$ and the line search hyperparameter is $\beta = \frac{1}{2}$ in all the experiments. The attempt value for the steplength at Step 2 is, in general, $\alpha_0 = 1$ for the first iteration, and $\alpha_k = \min(\alpha_0, \alpha_{k-1}\frac{1}{\beta})$ for the following iterations. Furthermore we have the rule $\varepsilon_k = 100 \cdot 0.999^k$ for the control of the variance.

Method	Loss	α	$\overline{N}$	m
MNIST	LR	α_{opt}	1	2N
MNIST	NN	0.05	256	$\frac{2N}{256}$
w8a	LR	0.05	256	$\frac{2N}{256}$
w8a	NN	0.05	256	$\frac{2N}{256}$
IJCNN	LR	α_{opt}	1	2N
IJCNN	NN	α_{opt}	1	2N
RCV1	LR	α_{opt}	1	2N
RCV1	NN	α_{opt}	1	2N

Table 11: Settings for Prox-Spider-boost [45].